

ASSUMPTION-LEAN INFERENCE ON TREATMENT EFFECT DISTRIBUTIONS

005 **Anonymous authors**

006 Paper under double-blind review

ABSTRACT

011 In many fields, including healthcare, marketing, and online platform design, A/B
 012 tests are used to evaluate new treatments and make launch decisions based on aver-
 013 age treatment effect (ATE) estimates. But this workflow can overlook distributional
 014 risks, such as a large fraction of individuals affected negatively by the treatment.
 015 Prior work in this setting has estimated partial identification bounds—known as
 016 Makarov bounds—on the cumulative distribution function of the treatment effect
 017 by making restrictive assumptions on the outcome distribution. **In this paper,**
 018 **we propose a novel method for estimation and inference on Makarov bound that**
 019 **guarantees accurate estimation and valid asymptotic inference of the Makarov**
 020 **bounds for any outcome distribution under weaker assumptions.** Our main tech-
 021 nical contributions are to develop smoothed surrogates for the Makarov bounds,
 022 derive semiparametrically efficient estimators of these surrogates, and propose a
 023 procedure for optimal selection of the smoothing parameters. We show empirically
 024 on synthetic and semi-synthetic datasets that, by not relying on the assumptions
 025 made by other methods, our estimators achieve a better bias-variance trade-off and
 026 lower mean-squared error. Finally, we deploy our method on real A/B test data
 027 from a large social media platform, and show how estimates of the treatment effect
 028 distribution can inform decision-making.

1 INTRODUCTION

031 Randomized controlled trials (RCTs) and A/B tests are crucial for evaluating the impact of treatments
 032 or product changes on a target outcome. Examples include medical treatments aimed at improving
 033 patient health (Feuerriegel et al., 2024), advertising placement to increase revenue (Varian, 2016),
 034 and interventions on digital platforms to boost user engagement (Swaminathan & Joachims, 2015).
 035 By randomly assigning units to treatment and control, A/B tests enable unbiased comparisons of
 036 outcomes between groups. A common decision rule is to estimate the *average treatment effect* (ATE)
 037 and adopt the new treatment when the ATE is statistically significantly positive (Athey et al., 2020).
 038

039 In many settings, the ATE is not sufficient for decision-making and practitioners in fact need estimates
 040 of distributional quantities beyond the average (Kallus & Zhou, 2021). In sensitive applications it is
 041 vital to understand the fraction of individuals that are affected negatively by the treatment, even when
 042 the average treatment effect is positive. For example, a minor tweak to a platform’s ranking algorithm
 043 may lift overall engagement yet reduce engagement for new or low-activity users, increasing early
 044 churn. Such business-critical decisions motivate estimating the *entire distribution of the treatment*
 045 *effect*, rather than merely the mean.

046 Estimating the treatment effect distribution is challenging. Even in RCTs, where randomization rules
 047 out unobserved confounding, the joint distribution of potential outcomes is not identified (Fan &
 048 Park, 2010). Consequently, the treatment-effect distribution is only *partially* identified: its cumulative
 049 distribution function (c.d.f.) is bounded by the sharp *Makarov bounds* (Makarov, 1982). These
 050 bounds are obtained by optimizing over all possible joint distributions of treatment and control that
 051 are consistent with the the observed marginal distributions of treatment and control. Hence the
 052 Makarov bounds are complex functionals of the data-generating distribution that involve suprema
 053 and infima over the outcome space. The non-smoothness of these suprema and infima complicates
 estimation of the bounds and especially complicates the application of standard tools from efficiency
 theory, such as debiased estimation (Kennedy, 2022).

Existing methods for efficient statistical inference on Makarov bounds either address stylized settings, such as a binary outcome (Kallus et al., 2022; Zhang & Richardson, 2025), or rely on a *margin assumption* (Semenova, 2025). The margin assumption requires the suprema and infima in the Makarov bounds to be attained at unique points, and is often violated in practice. **For example, if the treatment effect is constant or nearly constant for a subset of users, the margin assumption will fail or nearly fail to hold. This naturally occurs when outcomes are discrete or exhibit zero inflation, which is a common occurrence in applied work.** In this case, existing estimators are biased or high-variance, leading to inaccurate estimates and sub-optimal decisions.

In this paper, we propose a novel, assumption-lean, method for inference on Makarov bounds for the treatment-effect distribution. Our key idea is to replace the non-smooth suprema and infima that define the bounds with smooth surrogates, allowing us to apply semiparametric efficiency theory to obtain debiased estimators. We then derive an upper bound on the bias introduced by smoothing and incorporate it into both the selection of the smoothing parameters and the construction of our confidence intervals. Our method offers three key advantages: (i) it provides lower mean-squared error (MSE) estimates of Makarov bounds under violation of the margin assumption; (ii) it is model-agnostic and can be combined with arbitrary black-box learners to exploit covariates and tighten the bounds; and (iii) it admits data-driven procedures for selecting the smoothing level optimally.

Our contributions are¹: (i) We propose debiased estimators of smoothed versions of the Makarov bounds and quantify the induced smoothing bias; (ii) We propose a new data-driven procedure to tune the smoothing parameters of our method; and (iii) We validate the effectiveness of our method using synthetic, semi-synthetic, and real-world data.

2 RELATED WORK

Quantile treatment effects. One stream of literature focuses on estimating quantile treatment effects (QTEs) (Abadie & Angrist, 1998; Chernozhukov & Hansen, 2005; Firpo, 2007). These are contrasts of quantiles of the potential outcomes distributions, defined via

$$\text{QTE}(\tau) = F_{Y(1)}^{-1}(\tau) - F_{Y(0)}^{-1}(\tau),$$

which compares the τ -quantile of $Y(1)$ to the τ -quantile of $Y(0)$. Note that QTEs do not quantify quantiles of the treatment effect distribution: QTEs describe how treatment shifts the marginal distributions of potential outcomes across individuals (for example, how the τ -quantile under treatment differs from the τ -quantile under control), while the latter would characterize the distribution of individual-level causal effects $Y(1) - Y(0)$ in the population. In contrast to QTEs, the treatment effect distribution is generally not identifiable from observed data without additional assumptions, and is the focus of our paper.

Distributions of treatment effects. There are two main streams of work on statistical inference for treatment-effect distributions. The first stream aims at constructing *prediction intervals* for the individual treatment effect (ITE), typically based on conformal prediction (Lei & Candès, 2021; Alaa et al., 2023; Schröder et al., 2024). These methods provide valid predictive intervals for individual-level effects, but do not allow for inference on the full treatment-effect distribution (e.g., estimating its c.d.f. or density).

The second stream focuses on inference on the c.d.f. of the treatment-effect distribution. However, this distribution is not identifiable under standard assumptions (Rubin, 1974; Robins, 1986; Fan & Park, 2010), even with experimental data. Two approaches to overcome this obstacle have emerged. The first is to impose additional assumptions on the data-generating process to achieve point identification, as in Post & Van Den Heuvel (2025). Such assumptions, however, are unrealistic and untestable. The second is to take a partial identification approach and estimate upper and lower *bounds* on the cumulative distribution function. For example, sharp bounds and corresponding estimators have been proposed for binary outcomes (Kallus et al., 2022; Zhang & Richardson, 2025).

For general outcomes, sharp bounds are given by the Makarov bounds (Makarov, 1982). Estimation and inference methods for these bounds are mostly based on *plug-in* approaches (Fan & Park, 2010; Ruiz & Padilla, 2022; Fava, 2024; Lee, 2024; Cui & Han, 2023; Liang & Wu, 2025), which do

¹Code: <https://anonymous.4open.science/r/SmoothedMakarovBounds-632B>.

not leverage semiparametric efficiency theory (Kennedy, 2022). The resulting estimators are not guaranteed to be asymptotically normal and confidence intervals are often constructed via invalid bootstrap procedures. Beyond Makarov bounds, Firpo & Ridder (2019) introduced uniformly sharp bounds for the treatment-effect distribution, but these are computationally challenging as no closed-form expressions are available. Similarly, Ji et al. (2023) proposed a dual-optimization framework for partial identification, but this framework can yield overly conservative bounds when strong duality fails (see their Sec. 6.2).

Efficient estimation of non-smooth causal estimands. A key technical difficulty in the estimation of the Makarov bounds is that the bounds involve suprema and infima over the outcome space. These suprema and infima are non-differentiable, precluding the use of standard theory.

One literature stream attempts to remedy this by making a so-called *margin assumption* (Kitagawa & Tetenov, 2018), which essentially requires that the suprema and infima are attained at a single point only. This assumption has been used in the estimation of various other statistical estimands with similar non-differentiability issues: the optimal policy value (Luedtke & Van Der Laan, 2016), covariate-conditional Makarov bounds (Melnychuk et al., 2024), and more general intersection bounds (Semenova, 2025) which include Makarov bounds as a special case. However, the margin assumption is violated even in simple settings, like that of a constant treatment effect, making these methods unreliable in practice.

A second stream of work handles non-differentiability by approximating non-differentiable functions (e.g., the supremum) with smooth functions. This approach has been developed for inference on the optimal policy value Park (2024) and on bounds on average treatment effects in instrumental variable settings Levis et al. (2025). To the best of our knowledge no prior work has proposed a similar method for estimation and inference of Makarov bounds, which is the scope of our paper.

3 PROBLEM SETUP

3.1 SETTING

Data: We consider a causal inference setting using either randomized or observational data. That is, we consider a population $Z = (X, A, Y) \sim \mathbb{P}$, where $X \in \mathcal{X} \subseteq \mathbb{R}^d$ are covariates, $A \in \{0, 1\}$ is a binary action, and $Y \in \mathbb{R}$ is a continuous outcome of interest that is observed after taking the action A . For example, X may be user demographics, A may be a binary decision of whether a policy is implemented, and Y may be a user engagement metric. We provide extensions of all our results to discrete outcomes in Appendix C. We also assume that we have access to a dataset $\mathcal{D} = \{(x_i, a_i, y_i)\}_{i=1}^n$ of size $n \in \mathbb{N}$ sampled i.i.d. from \mathbb{P} .

Notation. We define the *propensity score* as $\pi(x) = \mathbb{P}(A = 1 \mid X = x)$. The propensity score characterizes the treatment assignment mechanism and is often known in randomized experiments, e.g., $\pi(x) = 0.5$. Furthermore, we define the *response distributions* as the conditional outcome c.d.f.s $F_a(y|x) = \mathbb{P}(Y \leq y \mid X = x, A = a)$ for $a \in \{0, 1\}$. We let $\eta = \{\pi, F_1, F_0\}$ be the collection of these *nuisance functions*. For any $v \in \mathbb{R}$, we write $v_+ = \max(v, 0)$ and $v_- = \min(v, 0)$.

Target estimand. We use the potential outcomes framework of Rubin (1974) and denote $Y(a)$ as the potential outcome corresponding to the treatment $A = a$. The parameter of interest is the cumulative distribution function of the treatment effect evaluated at a single point,

$$\rho(\delta) = \mathbb{P}(Y(1) - Y(0) \leq \delta). \quad (1)$$

The c.d.f. $\rho(\delta)$ characterizes the entire treatment effect distribution. For example, $\rho(0)$ is the fraction of users negatively affected by the treatment (Kallus et al., 2022).

162 **Partial identification bounds.** We impose the following standard causal inference assumptions
 163 (Rubin, 1974).

164 **Assumption 3.1** (Standard causal inference assumptions). For all $a \in \{0, 1\}$ and $x \in \mathcal{X}$ we have:
 165 (i) *consistency*, $Y(a) = Y$ whenever $A = a$; (ii) *overlap*, $0 < \pi(x) < 1$ whenever $\mathbb{P}(X = x) > 0$;
 166 and (iii) *ignorability*, $A \perp Y(1), Y(0) \mid X = x$.

167 Conditions (ii) and (iii) are automatically satisfied in randomized experiments where the propensity
 168 score π is known and can be controlled (and is often the constant function $\pi(x) = 0.5$). Condition (i)
 169 prohibits interference between individuals and excludes the possibility of spillover effects. Together,
 170 these assumptions allow us to *partially identify* the treatment effect distribution $\rho(\delta)$ via the Makarov
 171 bounds (Makarov, 1982)

$$173 \quad \rho^-(\delta) \leq \rho(\delta) \leq \rho^+(\delta), \quad (2)$$

174 where

$$175 \quad \rho^-(\delta) = \mathbb{E} \left[\sup_{y \in \mathcal{Y}} (F_1(y|X) - F_0(y - \delta|X))_+ \right] \text{ and } \rho^+(\delta) = 1 + \mathbb{E} \left[\inf_{y \in \mathcal{Y}} (F_1(y|X) - F_0(y - \delta|X))_- \right]. \quad (3)$$

176 The Makarov bounds $\rho^-(\delta)$ and $\rho^+(\delta)$ only depend on the marginal response distributions F_1 and F_0
 177 and are thus identified from the observation distribution \mathbb{P} . Intuitively, the Makarov bounds quantify
 178 the stochastically smallest and largest distributions that can be obtained by maximizing or minimizing
 179 over joint distributions of the potential outcomes that are compatible with the observed marginals
 180 F_1 and F_0 . (They are also generalizations of the bounds from (Kallus, 2022) for the fraction of
 181 negatively affected users in the case of binary outcomes.)

185 3.2 BACKGROUND ON ESTIMATING MAKAROV BOUNDS

186 **Plug-in estimation.** The simplest estimator of the Makarov bounds is the so-called *plug-in estimator*
 187 (Fan & Park, 2010): one first obtains nuisance estimators $\hat{\eta} = (\hat{F}_1, \hat{F}_0, \hat{\pi})$ of the response distributions
 188 F_a and propensity score π (in the observational setting). Then, one substitutes the estimated nuisance
 189 functions into the expression for the bound from Eq. (3) to obtain

$$191 \quad \hat{\rho}_{\text{PI}}^-(\delta) = \frac{1}{n} \sum_{i=1}^n \sup_{y \in \mathcal{Y}} \left(\hat{F}_1(y|x_i) - \hat{F}_0(y - \delta|x_i) \right)_+. \quad (4)$$

194 However, it turns out that the plugin estimator $\hat{\rho}_{\text{PI}}^-(\delta)$ has two drawbacks (Kennedy, 2022): (i) plug-in
 195 bias, which makes it asymptotically suboptimal, and (ii) difficulty establishing asymptotic normality
 196 under reasonable conditions on the nuisance estimators, which prevents reliable confidence interval
 197 construction.

198 **Semiparametric efficient estimators.** To address these limitations, a major line of work in causal
 199 inference leverages *semiparametric efficiency theory* to construct *debiased estimators*. Debiased
 200 estimators are of the form

$$202 \quad \hat{\rho}_{\text{A IPTW}}^-(\delta) = \hat{\rho}_{\text{PI}}^-(\delta) + \frac{1}{n} \sum_{i=1}^n \Psi_{\delta, y^*}^-(z_i, \hat{\eta}, \hat{\rho}_{\text{PI}}^-(\delta)), \quad (5)$$

205 where $\Psi_{\delta, y^*}^-(Z, \eta, \rho^-(\delta))$ is the so-called *efficient influence function* (EIF) of the target estimand.
 206 Adding the EIF term debiases the plug-in estimator, yielding an estimator that is asymptotically
 207 efficient and normally distributed, i.e., yielding the lowest possible asymptotic variance given
 208 by $\mathbb{E}[\Psi_{\delta, y^*}^-(Z, \eta, \rho^-(\delta))^2]$. Hence, debiasing using the EIF enables valid and efficient statistical
 209 inference.

210 **Envelope estimators for Makarov bounds.** For the lower Makarov bound, the efficient influence
 211 function is given by (Melnichuk et al., 2024; Semenova, 2025):

$$213 \quad \Psi_{\delta, y^*}^-(Z, \eta, \rho^-(\delta)) = d_{\delta, \eta}(y^*|X) - \rho^-(\delta) + \mathbf{1}(d_{\delta, \eta}(y^*|X) > 0) \left(\frac{A}{\pi(X)} (1(Y \leq y^*) - F_1(y^*|X)) \right. \quad (6)$$

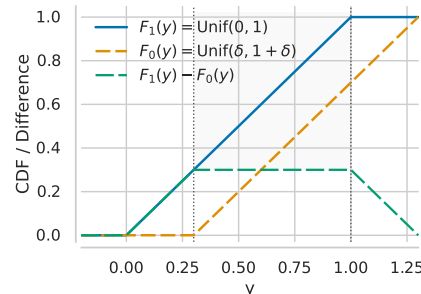
$$215 \quad \left. - \frac{1-A}{1-\pi(X)} (1(Y \leq y^* - \delta) - F_0(y^* - \delta|X)) \right), \quad (7)$$

216 where $d_{\delta,\eta}(y|X) = F_1(y|X) - F_0(y - \delta|X)$ and $y^* \in \arg \max_{y \in \mathcal{Y}} d_{\delta,\eta}(y|X)$.
 217

218 For each observation x_i , y^* can be computed (e.g., via grid search) and plugged into the debiased
 219 estimator from Eq. (5). This approach is known as an *envelope estimator* (Semenova, 2025).

220 **Margin assumption.** Debiased estimators rely on several
 221 assumptions, including pathwise differentiability (van der
 222 Laan & Rubin, 2006). For Makarov bounds, this
 223 essentially translates to requiring the supremum and infimum
 224 y^* to yield unique solutions, which is known as the *margin
 225 assumption* (Kitagawa & Tetenov, 2018). However, this
 226 assumption is violated even for the simple case of con-
 227 stant treatment effects for a subset of users. Indeed, if the
 228 treatment effect is constant for users with some values of
 229 X , then the treatment c.d.f. $F_1(y|X)$ for these users is
 230 a constant vertical shift of the control c.d.f. $F_0(y|X)$,
 231 and the supremum/ infimum y^* can be attained at many
 232 values of y (see Fig. 1 for an illustration). **Importantly,**
 233 **such (near-) constant effects are not just a feature of styl-
 234 ized toy examples. They naturally occur when outcomes
 235 are discrete or exhibit zero inflation, which is a common
 236 occurrence in applied work. For instance, in A/B tests with binary or highly skewed outcomes such as
 237 clicks, conversions, or purchases (many units with exactly zero events).** Thus, the margin assumption
 238 fails and the envelope estimator is no longer efficient. This inefficiency can manifest a sub-optimal
 239 mean-squared-error, because the margin assumption can inflate the variance of the estimator which
 240 can lead to suboptimal bias-variance trade-off as we will show later.

241 We emphasize that the failure of the margin assumption is not restricted to pathological edge cases.
 242 Constant treatment effects are a basic model of causal inference, and since effect sizes are often
 243 extremely small in digital experiments, we are often very nearly in the setting of a constant zero
 244 treatment effect. We cannot confidently use estimators that rely on a margin assumption when
 245 analyzing real-world data, necessitating the development of new methods.



246 **Figure 1: Example for violating the**
 247 **margin assumption.** Depicted are two
 248 shifted (uniform) c.d.f.s that violate the
 249 margin assumption, leading to a plateau
 250 where the argmax is not unique.

251 **4 ESTIMATING MAKAROV BOUNDS IN THE PRESENCE OF MARGIN
 252 VIOLATIONS**

253 In this section, we present our methodology for valid inference on Makarov bounds when the margin
 254 assumption is violated. Our strategy proceeds in three steps. First, in Sec.4.1, we introduce a smooth
 255 surrogate approximation of the Makarov bounds that is amenable to debiased estimation. Next, in
 256 Sec.4.2, we derive debiased estimators for these smoothed bounds and construct confidence intervals
 257 that achieve valid coverage. Finally, in Sec. 4.3, we propose a data-driven procedure to select the
 258 smoothing parameters in a principled way.

259 4.1 A SMOOTH APPROXIMATION FOR THE MAKAROV BOUNDS

260 Two key components of the Makarov bounds in Eq. (3) prevent debiased inference in the presence
 261 of margin violations: (i) the supremum and infimum operators, $\sup_{y \in \mathcal{Y}}$ and $\inf_{y \in \mathcal{Y}}$, and (ii) the
 262 positivity and negativity operators, $(\cdot)_+ = \max(\cdot, 0)$ and $(\cdot)_- = \min(\cdot, 0)$. Both components
 263 are non-smooth in the presence of margin violations. Intuitively, when the optimizer has multiple
 264 solutions, even small estimation errors in the nuisance functions can lead to large and unstable
 265 variation in the estimator, as well as bias in the wrong direction. This instability is what invalidates
 266 asymptotic efficiency and reliable confidence intervals.

267 **Bound approximations.** Our key idea is to replace these problematic components with smooth
 268 approximations that return unique values, even when the original functions are flat or multi-valued.
 269 This smoothing restores pathwise differentiability, enabling debiased estimation and valid inference
 270 without requiring the margin assumption. For the suprema and infima, we adapt the approximation
 271 from (Levis et al., 2025) for discrete maxima to continuous variables and define the continuous

270 log-sum-exp operator (LSE) $g_{t_1} : \mathcal{F} \rightarrow \mathbb{R}$ via
 271

$$272 \quad g_{t_1}(f) = \frac{1}{t_1} \log \left(\int \exp(t_1 f(y)) dy \right) \quad (8)$$

273 For (ii), we replace v_+ and v_- with the softplus function $h_{t_2} : \mathbb{R} \rightarrow \mathbb{R}$ via $h_{t_2}(u) = \frac{1}{t_2} \log(1 + e^{t_2 u})$.
 274 The following lemma shows that replacing the components in (i) and (ii) with g_{t_1} and h_{t_2} gives good
 275 approximations of the Makarov bounds.

276 **Lemma 4.1** (Makarov bound approximations). *Assume that \mathcal{Y} is compact with finite Lebesgue
 277 measure $|\mathcal{Y}|$. For any $t_1, t_2 > 0$, we define the smoothed Makarov bounds via*

$$278 \quad \rho_{t_1, t_2}^-(\delta) = \mathbb{E} \left[\frac{1}{t_2} \log \left(1 + I_{t_1, \delta}(X)^{\frac{t_2}{t_1}} \right) \right] \text{ and } \rho_{t_1, t_2}^+(\delta) = 1 - \mathbb{E} \left[\frac{1}{t_2} \log \left(1 + I_{-t_1, \delta}(X)^{\frac{t_2}{t_1}} \right) \right], \quad (9)$$

278 where

$$279 \quad I_{t, \delta}(x) = \int_{\mathcal{Y}} \exp(t[F_1(y|x) - F_0(y - \delta|x)]) dy. \quad (10)$$

280 Then, it holds that

$$281 \quad \rho_{t_1, t_2}^-(\delta) - b(t_1, t_2) \leq \rho^-(\delta) \text{ and } \rho_{t_1, t_2}^+(\delta) \leq \rho_{t_1, t_2}^+(\delta) + b(t_1, t_2), \quad (11)$$

282 where $b(t_1, t_2) = \frac{\log(2)}{t_2} + \frac{(\log|\mathcal{Y}|)_+}{t_1}$ quantifies the approximation bias. Furthermore, $\rho_{t_1, t_2}^-(\delta) \rightarrow$
 283 $\rho^-(\delta)$ and $\rho_{t_1, t_2}^+(\delta) \rightarrow \rho^+(\delta)$ as $t_1, t_2 \rightarrow \infty$.

284 *Proof.* See Appendix A. □

285 Intuitively, this smoothing replaces the “hard max” operation of the supremum with a “soft max.”
 286 Instead of arbitrarily selecting one of multiple equally optimal points, the approximation takes a
 287 smooth weighted average that changes gradually as the nuisance estimates shift. This makes the
 288 estimator more stable and allows for establishing asymptotic normality of debiased estimators.

289 4.2 DEBIASED ESTIMATORS

300 We now derive the debiased estimators for the smoothed bounds in Lemma 4.1. The following result
 301 establishes the efficient influence functions (EIF) of the lower and upper approximation.

302 **Theorem 4.2.** *The efficient influence functions of the smoothed Makarov bounds $\rho_{t_1, t_2}^-(\delta)$ and
 303 $\rho_{t_1, t_2}^+(\delta)$ are given by*

$$304 \quad \Psi_{t_1, t_2, \delta}^-(Z, \eta, \rho_{t_1, t_2}^-(\delta)) = \sigma_{t_1, t_2, \delta}^-(X) \left[\frac{A}{\pi(X)} \Phi_{t_1, \delta}^1(X, Y) - \frac{1-A}{1-\pi(X)} \Phi_{t_1, \delta}^0(X, Y) \right] \quad (12)$$

$$305 \quad + \frac{1}{t_2} \log \left(1 + I_{t_1, \delta}(X)^{\frac{t_2}{t_1}} \right) - \rho_{t_1, t_2}^-(\delta), \quad (13)$$

$$306 \quad \Psi_{t_1, t_2, \delta}^+(Z, \eta, \rho_{t_1, t_2}^+(\delta)) = \sigma_{t_1, t_2, \delta}^+(X) \left[\frac{A}{\pi(X)} \Phi_{-t_1, \delta}^1(X, Y) - \frac{1-A}{1-\pi(X)} \Phi_{-t_1, \delta}^0(X, Y) \right] \quad (14)$$

$$307 \quad + 1 - \frac{1}{t_2} \log \left(1 + I_{-t_1, \delta}(X)^{\frac{t_2}{t_1}} \right) - \rho_{t_1, t_2}^+(\delta), \quad (15)$$

308 where we denote

$$309 \quad \Phi_{t_1, \delta}^a(X, Y) = \int_{\mathcal{Y}} w_{t_1, \delta}(y | X) \left(\mathbf{1}\{Y \leq y - (1-a)\delta\} - F_a(y - (1-a)\delta | X) \right) dy, \quad (16)$$

$$310 \quad w_{t_1, \delta}(y | x) = \frac{\exp(t_1(F_1(y|x) - F_0(y - \delta|x)))}{I_{t_1, \delta}(x)}, \quad (17)$$

$$311 \quad \sigma_{t_1, t_2, \delta}^-(x) = \frac{I_{t_1, \delta}(x)^{t_2/t_1}}{1 + I_{t_1, \delta}(x)^{t_2/t_1}}, \text{ and } \sigma_{t_1, t_2, \delta}^+(x) = \frac{I_{-t_1, \delta}(x)^{t_2/t_1}}{1 + I_{-t_1, \delta}(x)^{t_2/t_1}}. \quad (18)$$

324 *Proof.* See Appendix A. □

326
 327 The smoothed EIFs from Theorem 4.2 are of similar structure as the envelope EIF from Eq. (6).
 328 Crucially however, the terms involving the argmax/argmin y^* are replaced by smooth weighted
 329 integrals $\Phi_{t_1,\delta}^a(X, Y)$, and the indicator $\mathbf{1}(d_{\delta,\eta}(y^*|X) > 0)$ is replaced with one of the smooth
 330 approximations $\sigma_{t_1,t_2,\delta}^{\pm}(X)$.

331 Using Theorem 4.2, we can now obtain debiased estimators for the smoothed Makarov bounds.
 332 Following Eq. (5), these are given by

333

$$\hat{\rho}_{t_1,t_2}^-(\delta) = \frac{1}{n} \sum_{i=1}^n \frac{1}{t_2} \log \left(1 + \hat{I}_{t_1,\delta}(x_i)^{\frac{t_2}{t_1}} \right) + \hat{\sigma}_{t_1,t_2,\delta}^-(x_i) \left[\frac{a_i - \hat{\pi}(x_i)}{\hat{\pi}(x_i)(1 - \hat{\pi}(x_i))} \hat{\Phi}_{t_1,\delta}^{a_i}(x_i, y_i) \right], \quad (19)$$

334

$$\hat{\rho}_{t_1,t_2}^+(\delta) = \frac{1}{n} \sum_{i=1}^n 1 - \frac{1}{t_2} \log \left(1 + \hat{I}_{-t_1,\delta}(x_i)^{\frac{t_2}{t_1}} \right) + \hat{\sigma}_{t_1,t_2,\delta}^+(x_i) \left[\frac{a_i - \hat{\pi}(x_i)}{\hat{\pi}(x_i)(1 - \hat{\pi}(x_i))} \hat{\Phi}_{-t_1,\delta}^{a_i}(x_i, y_i) \right].$$

335

341 **Correcting for approximation bias.** Using above debiased estimators enables efficient and asymptotically normal inference, and thus construction of confidence intervals for the smoothed Makarov
 342 bounds. However, it remains to translate these intervals to the non-smoothed Makarov bounds,
 343 as the smoothing may introduce bias. Luckily, we can leverage Lemma 4.1 to upper bound this
 344 approximation bias via the term $b(t_1, t_2)$. We can then add this term to the one-sided confidence
 345 intervals for the upper and lower Makarov bounds, yielding valid confidence intervals as follows.

346 **Corollary 4.3** (Asymptotic confidence interval for the treatment effect distribution). *Assume the
 347 nuisance estimators $\hat{\eta}$ are obtained on an independent sample from \mathcal{D} (e.g., via sample splitting or
 348 cross-fitting). Under standard regularity and rate conditions for orthogonal/debiased estimation (e.g.,
 349 Chernozhukov et al., 2018), it holds for each fixed δ that*

350

$$\lim_{n \rightarrow \infty} \mathbb{P} \left(c_{t_1,t_2,\delta,\alpha}^-(\mathcal{D}_n) \leq \rho(\delta) \leq c_{t_1,t_2,\delta,\alpha}^+(\mathcal{D}_n) \right) \geq 1 - \alpha, \quad (20)$$

351

352 where

353

$$c_{t_1,t_2,\delta,\alpha}^{\pm}(\mathcal{D}_n) = \hat{\rho}_{t_1,t_2}^{\pm}(\delta) \pm z_{1-\alpha/2} \sqrt{\frac{1}{n^2} \sum_{i=1}^n \left(\Psi_{t_1,t_2,\delta}^{\pm}(z_i, \hat{\eta}, \hat{\rho}_{t_1,t_2}^{\pm}(\delta)) \right)^2} \pm b(t_1, t_2), \quad (21)$$

354

355 $b(t_1, t_2)$ is from Lemma 4.1, $\Psi_{t_1,t_2,\delta}^{\pm}$ are given in Theorem 4.2, and $z_{1-\frac{\alpha}{2}}$ denotes the $1 - \frac{\alpha}{2}$ standard
 356 normal quantile.

362 *Proof.* See Appendix A. □

364 4.3 SMOOTHING PARAMETER SELECTION

366 **Bias-variance trade-off.** Our smoothed debiased estimators from Eq. (19) depend on the smoothing
 367 parameters t_1 and t_2 that quantify the approximation quality of the non-smooth bound components.
 368 This implies a trade-off between the approximation-induced bias and the variance reduction under
 369 margin violation. Formally, a standard MSE decomposition yields

370

$$\mathbb{E}_n [(\hat{\rho}_{t_1,t_2}^-(\delta) - \rho^-(\delta))^2] = \underbrace{(\hat{\rho}_{t_1,t_2}^-(\delta) - \rho^-(\delta))^2}_{\text{approximation (smoothing) bias}^2} + \underbrace{\frac{1}{n} \mathbb{E} [\Psi_{t_1,t_2,\delta}^-(Z, \eta, \hat{\rho}_{t_1,t_2}^-(\delta))^2]}_{\text{asymptotic variance}/n} + \underbrace{o\left(\frac{1}{n}\right)}_{\text{remainder}}. \quad (22)$$

371

375 As a consequence, choosing the smoothing parameters t_1 and t_2 correctly is crucial to obtain a low
 376 MSE that optimizes the bias-variance trade-off. We propose two different methods for data-driven
 377 smoothing-parameter selection: (i) minimizing an upper bound on the MSE, and (ii) using Lepski's
 378 method. Our full proposed procedure is shown in Algorithm 1.

378 **Algorithm 1:** Smoothed estimation of
 379 Makarov bounds with sample splitting.

380 1: **Input:** Dataset $\mathcal{D} = \{(x_i, a_i, y_i)\}_{i=1}^n$
 381 2: **Stage 0:** Split the data \mathcal{D} randomly into two
 382 disjoint datasets \mathcal{D}_1 and \mathcal{D}_2 .
 383 3: **Stage 1a:** Estimate nuisance functions
 $\hat{\eta} = (\hat{F}_1, \hat{F}_0, \hat{\pi})$ on \mathcal{D}_1 ; obtain predictions on \mathcal{D}_2 .
 384 4: **Stage 1b:** Obtain tuned smoothing parameters \hat{t}_1^\pm
 385 and \hat{t}_2^\pm on \mathcal{D}_1 .
 386 5: **Stage 2:** Compute debiased estimators $\hat{\rho}_{\hat{t}_1^\pm, \hat{t}_2^\pm}^-(\delta)$
 387 and $\hat{\rho}_{\hat{t}_1^\pm, \hat{t}_2^\pm}^+(\delta)$.
 388 6: **Output:** g_θ and α_ϕ .

390 bias without paying unnecessary variance. We start by ranking all candidate pairs $(t_1^{(k)}, t_2^{(k)})$ within
 391 the grid by the size of their associated bias term $B_k = b(t_1^{(k)}, t_2^{(k)})$ in *descending* order (more smooth-
 392 ing first). Scanning in this order, for each k compare the corresponding estimates $\hat{\rho}_{t_1^{(k)}, t_2^{(k)}}^-(\delta)$
 393 to a small set of less-smoothed candidates r with $B_r < B_k$ and accept the first k such that
 394 $|\hat{\rho}_{t_1^{(k)}, t_2^{(k)}}^-(\delta) - \hat{\rho}_{t_1^{(r)}, t_2^{(r)}}^-(\delta)| \leq z_{1-\alpha/2} \widehat{\text{SE}}(k, r)$ for all such r , where the tolerance uses EIF
 395 differences $\widehat{\text{SE}}(k, r) = 1/\sqrt{n} \text{sd}_n \left(\widehat{\Psi}_{t_1^{(k)}, t_2^{(k)}, \delta}^-(Z_i, \hat{\eta}, \hat{\rho}_{t_1^{(k)}, t_2^{(k)}}^-(\delta)) - \widehat{\Psi}_{t_1^{(r)}, t_2^{(r)}, \delta}^-(Z_i, \hat{\eta}, \hat{\rho}_{t_1^{(r)}, t_2^{(r)}}^-(\delta)) \right)$,
 396 and $\text{sd}_n(\cdot)$ is the empirical standard deviation over $i = 1, \dots, n$.
 397

5 EXPERIMENTS

400 We now confirm the effectiveness of our proposed method empirically. As is standard in causal
 401 inference (Shalit et al., 2017; Curth & van der Schaar, 2021), we evaluate our method on synthetic and
 402 semi-synthetic data where we have access to ground-truth values of causal quantities. We also provide
 403 experimental results using real-world A/B tests. Additional experimental results are in Appendix I.

404 **Nuisance estimation.** We estimate the treatment-specific conditional c.d.f.s $F_a(\cdot | x)$, $a \in \{0, 1\}$, via
 405 likelihood-based gradient boosting with sample-splitting. For continuous outcomes we fit covariate-
 406 dependent Gaussian mixtures; for discrete outcomes we use a multinomial classifier and obtain the
 407 c.d.f. by cumulatively summing predicted class probabilities; and for nonnegative counts with excess
 408 zeros we employ a zero-inflated Poisson with covariate-dependent rate and zero-inflation. Training
 409 uses early stopping on held-out log-likelihood. Each learner outputs $\hat{F}_a(y | x)$ on an arbitrary grid in
 410 \mathcal{Y} of size $k = 300$ that is used for numerical integration. Details are in Appendix F.

411 **Baselines.** We compare our method with the *plug-in estimator* from Eq.(4) and the *envelope estimator*
 412 from Eq. (6). To ensure a fair comparison, we use the same nuisance estimators for $F_1(y|x)$ and
 413 $F_0(y|x)$ from above. Additionally, we also report results for our method and the baselines targeting
 414 the *marginal* Makarov bounds (corresponding to not using any covariates X). For the marginal
 415 bounds, we use the standard empirical c.d.f. on a holdout dataset as a nuisance estimator. We use
 416 Lepski's method for selecting the smoothing parameters.

417 **Evaluation.** For synthetic data with available ground-truth we report the estimation error $|\rho^\pm(\delta) -$
 418 $\hat{\rho}^\pm(\delta)|$ averaged over $K = 2500$ Monte Carlo runs for both the lower and the upper Makarov bound.
 419 For real-world data without ground-truth we report the estimated bounds and confidence intervals.

420 5.1 (SEMI)-SYNTHETIC DATA

421 **Fully synthetic data.** We simulate data from a synthetic data-generating process (DGP) that violates
 422 the margin assumption by having a constant treatment effect for some users. This leads to plateaus
 423 like those in Fig.1 in the difference between the treatment and control c.d.f. (see Appendix G).

424 We consider two variations of this DGP: (i) a variation with a smaller plateau width corresponding
 425 to only small assumption violation, and (ii) a variation with a larger plateau width corresponding
 426 to larger assumption violation. A comparison of our method to existing methods for both of these
 427 DGPs, for both the upper and lower bounds, with and without covariates, is given in Table. 2 (top)

432	433	434	435	436	437	438	439	440	Small assumption violation			Large assumption violation					
									Data	Bound	Side	Plugin	Envelope	Ours	Plugin	Envelope	Ours
432	433	434	435	436	437	438	439	440	Synthetic	Marginal	lower	3.98 ± 0.11	2.00 ± 0.05	1.81 ± 0.04	5.59 ± 0.11	1.35 ± 0.08	0.82 ± 0.06
										upper	4.53 ± 0.11	1.99 ± 0.06	1.92 ± 0.05	5.55 ± 0.11	1.40 ± 0.08	0.83 ± 0.06	
									OHIE	Cov.-adjusted	lower	5.02 ± 0.12	1.86 ± 0.05	1.81 ± 0.04	6.42 ± 0.13	1.28 ± 0.07	0.90 ± 0.06
										upper	4.67 ± 0.11	1.93 ± 0.05	1.84 ± 0.04	6.29 ± 0.12	1.25 ± 0.07	0.86 ± 0.06	
432	433	434	435	436	437	438	439	440	OHIE	Marginal	lower	1.95 ± 0.06	1.21 ± 0.03	0.76 ± 0.02	2.22 ± 0.06	1.14 ± 0.03	0.77 ± 0.02
										upper	2.40 ± 0.07	1.46 ± 0.04	1.09 ± 0.03	2.52 ± 0.07	1.31 ± 0.04	0.97 ± 0.03	
									OHIE	Cov.-adjusted	lower	4.88 ± 0.09	1.46 ± 0.03	1.44 ± 0.03	4.71 ± 0.09	1.09 ± 0.03	1.00 ± 0.02
										upper	5.29 ± 0.09	1.50 ± 0.04	1.41 ± 0.03	4.31 ± 0.09	1.28 ± 0.03	1.08 ± 0.03	

Table 2: Average mean-squared error of estimators of $\rho(0)$ across settings. Error bars are 95% CIs across 2500 replications. Our method consistently attains the lowest mean-squared error.

and shows that our **method achieves the best estimation performance** across all bound types and settings. Furthermore, the gap between our estimator and the baselines widens under stronger margin violation, highlighting that our method efficiently handles these violations when the baselines do not.

Semi-synthetic data. For our semi-synthetic experiments, we use covariate data from the *Oregon health insurance experiment* (OHIE) (Finkelstein et al., 2012). The OHIE was a randomized experiment meant to assess the effect of health insurance on outcomes such as health or economic status (see Appendix H for details). We use the following covariates: age, gender, language, the number of emergency visits before the experiment, and the number of people the individual signed up with. We then simulate treatment and outcomes such that the margin assumption is violated. Again, we consider two different settings with different the severities of assumption violation. The results are shown in Table. 2 (bottom). Again, **our method achieves the best estimation performance** across all bound types and settings and the gap between the smoothing and envelope estimators widens when the degree of assumption violation increases.

5.2 REAL-WORLD DATA

A/B tests from a consumer technology company. Finally, we apply our method to three real A/B tests from a large consumer technology company. All three A/B tests have constant propensity score $\pi(x) = 0.5$ and have on the order of tens of millions of observations. The first experiment is an experiment that boosts certain content in a ranking context, and the outcome metric is a measure of engagement. The second experiment demotes certain content in a (different) ranking context, and the outcome metric is a (different) measure of engagement. The third experiment tests a treatment meant to increase visitation, and the outcome metric is a visitation metric. Basic statistics for these experiments are reported in Table 3. For each experiment, we estimate the Makarov bounds to obtain a partial identification region for the c.d.f. of the treatment effect.

Table 3: Experiment statistics summary.

	Sample size, n	% ATE	Upper bound on $\rho(-1)$ ^(*)
Exp. 1	≈ 30m	16.25%	0.37
Exp. 2	≈ 5m	-1.76%	0.76
Exp. 3	≈ 10m	0.45%	0.99

Sample sizes approximate millions (m). (*) Setting $\delta = -1$ implies negative treatment effect.

Results. The results are shown in Figure 2. For the first experiment, we see that the partial identification region is relatively narrow. We are confident that $\mathbb{P}(Y_i(1) - Y_i(0) \leq -1) = \mathbb{P}(Y_i(1) - Y_i(0) < 0)$ is no more than 0.25, meaning that there are very few users for whom

the treatment is decreasing engagement. Since we are confident this treatment does not negatively affect a significant fraction of users, and the ATE estimate in Table 3 is positive, this treatment would be safe to launch. (On the other hand, the vertical jump in the identification region at 0 and the high lower bound on $\mathbb{P}(Y_i(1) - Y_i(0) \leq 0)$ suggest that—despite the positive ATE estimate—the treatment is actually having no effect on most users, likely due to the dynamics of the ranking, meaning that we may want to search for more effective treatments.)

For the second experiment, the partial identification region is wider—our upper bound on $\mathbb{P}(Y_i(1) - Y_i(0) < 0)$ is now 0.74, suggesting that this treatment may in fact affect a majority of users negatively, and we should conduct further analysis before launching it. Finally, for the third experiment, the partial identification region is extremely wide: our upper bound on $\mathbb{P}(Y_i(1) - Y_i(0) < 0)$ is now 0.99, suggesting that this treatment could potentially have a negative effect on nearly all users, and would be inadvisable to launch. Note that this experiment has a positive average treatment effect, as seen in Table 3, and so this recommendation to not launch contradicts the standard decision-making process.

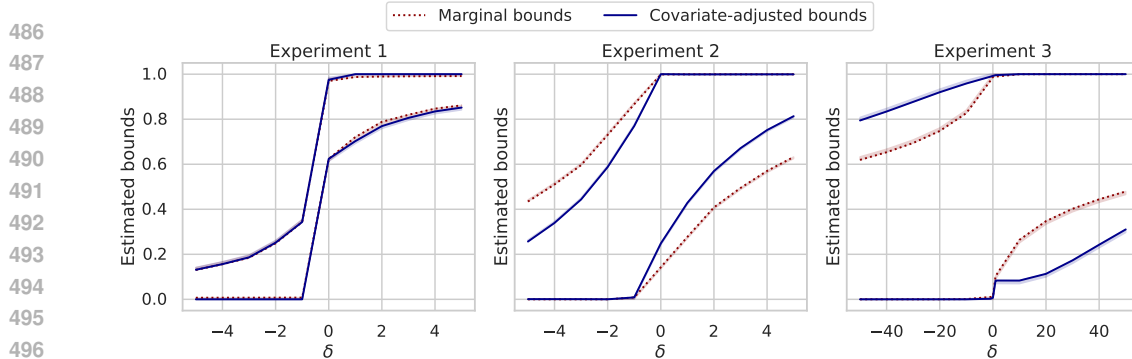


Figure 2: Estimated Makarov bounds for three A/B tests from a consumer technology company. Based on these bounds, we are confident that Experiment 1 does not negatively impact many users, and thus is safe to launch, whereas Experiments 2 and 3 may negatively impact many users.

Taken together, these three examples highlight how our methods can be used in real world settings to characterize treatment effect distributions more completely than the average treatment effect, and thus inform launch decisions. We also provide additional comparisons with baselines in Appendix I.

6 DISCUSSION.

In this paper, we proposed a new method for inferring Makarov bounds on the treatment effect distribution without making a margin assumption.

Limitations and future work. Our current approach is limited to static binary treatments. Future work may consider extending our approach to continuous or time-varying treatments and outcomes. Additionally, future work may also consider extensions to unbounded outcome spaces or settings with unit interference (common in A/B testing).

Broader impact. Our method enables practitioners to make inferences about treatment effect distribution without relying on untestable assumptions, thus improving the reliability of established methods.

Ethics statement. We adhere to the ICLR Code of Ethics and acknowledge this during submission. Our work analyzes synthetic, semi-synthetic, and anonymized A/B-test data; no personal data are released or re-identified. The methods aim to improve safety by quantifying the fraction potentially harmed, but misuse is possible; we therefore emphasize risk-aware reporting and recommend subgroup audits when sensitive attributes are used.

Reproducibility Statement. An anonymized repository (linked in the submission) provides code to train/evaluate our estimators, select smoothing parameters, and compute one-sided confidence intervals. The paper specifies assumptions and estimands (Problem Setup), the smoothing/bias bounds and EIF-based estimators (Method), and evaluation protocols (Experiments), with full proofs and additional details in the appendix. We release synthetic and semi-synthetic generators, document preprocessing, model classes, hyperparameters, seeds, and scripts to recreate all synthetic and semi-synthetic figures/tables. Proprietary A/B data cannot be shared, but we plan to release anonymized data and code upon acceptance.

540 REFERENCES
541

542 Alberto Abadie and Joshua Angrist. Instrumental variables estimation of quantile treatment effects,
543 1998.

544 Ahmed Alaa, Zaid Ahmad, and Mark van der Laan. Conformal meta-learners for predictive inference
545 of individual treatment effects. In *NeurIPS*, 2023.

546

547 Susan Athey, Raj Chetty, and Guido Imbens. Combining experimental and observational data to
548 estimate treatment effects on long term outcomes. *arXiv preprint*, arXiv:2006.09676, 2020.

549

550 Vahid Balazadeh, Vasilis Syrgkanis, and Rahul G. Krishnan. Partial identification of treatment effects
551 with implicit generative models. In *NeurIPS*, 2022.

552

553 Alexander Balke and Judea Pearl. Bounds on treatment effects from studies with imperfect compliance.
554 *Journal of the American Statistical Association*, 92(439):1171–1176, 1997.

555

556 Kan Chen, Bingkai Wang, and Dylan S. Small. A differential effect approach to partial identification
557 of treatment effects. *arXiv preprint*, arXiv:2303.06332, 2023.

558

559 Victor Chernozhukov and Christian Hansen. An iv model of quantile treatment effects. *Econometrica*,
560 73(1):245–261, 2005.

561

562 Victor Chernozhukov, Denis Chetverikov, Mert Demirer, Esther Duflo, Christian Hansen, Whitney
563 Newey, and James M. Robins. Double/debiased machine learning for treatment and structural
564 parameters. *The Econometrics Journal*, 21(1):C1–C68, 2018. ISSN 1368-4221.

565

566 Yifan Cui and Sukjin Han. Policy learning with distributional welfare. *arXiv preprint*
567 *arXiv:2311.15878*, 2023.

568

569 Alicia Curth and Mihaela van der Schaar. Nonparametric estimation of heterogeneous treatment
570 effects: From theory to learning algorithms. In *AISTATS*, 2021.

571

572 Jacob Dorn and Kevin Guo. Sharp sensitivity analysis for inverse propensity weighting via quantile
573 balancing. *Journal of the American Statistical Association*, 2022.

574

575 Jacob Dorn, Kevin Guo, and Nathan Kallus. Doubly-valid/ doubly-sharp sensitivity analysis for
576 causal inference with unmeasured confounding. *Journal of the American Statistical Association*,
577 2024.

578

579 Guilherme Duarte, Noam Finkelstein, Dean Knox, Jonathan Mummolo, and Ilya Shpitser. An
580 automated approach to causal inference in discrete settings. *Journal of the American Statistical
581 Association*, 2023.

582

583 Yanqin Fan and Sang Soo Park. Sharp bounds on the distribution of treatment effects and their
584 statistical inference. *Econometric Theory*, 26(3):931–951, 2010.

585

586 Bruno Fava. Predicting the distribution of treatment effects: A covariate-adjustment approach. *arXiv
587 preprint arXiv:2407.14635*, 2024.

588

589 Stefan Feuerriegel, Dennis Frauen, Valentyn Melnychuk, Jonas Schweisthal, Konstantin Hess, Alicia
590 Curth, Stefan Bauer, Niki Kilbertus, Isaac S. Kohane, and Mihaela van der Schaar. Causal machine
591 learning for predicting treatment outcomes. *Nature Medicine*, 2024.

592

593 Amy Finkelstein, Sarah Taubman, Bill Wright, Mira Bernstein, Jonathan Gruber, Joseph P. Newhouse,
594 Heidi Allen, and Katherine Baicker. The oregon health insurance experiment: Evidence from the
595 first year. *The Quarterly Journal of Economics*, 127(3):1057–1106, 2012.

596

597 Sergio Firpo. Efficient semiparametric estimation of quantile treatment effects. *Econometrica*, 75(1):
598 259–276, 2007.

599

600 Sergio Firpo and Geert Ridder. Partial identification of the treatment effect distribution and its
601 functionals. *Journal of Econometrics*, 213(1):210–234, 2019.

594 Dylan J. Foster and Vasilis Syrgkanis. Orthogonal statistical learning. *The Annals of Statistics*, 53(3):
 595 879–908, 2023. ISSN 0090-5364.

596

597 Dennis Frauen, Valentyn Melnychuk, and Stefan Feuerriegel. Sharp bounds for generalized causal
 598 sensitivity analysis. In *NeurIPS*, 2023.

599 Dennis Frauen, Fergus Imrie, Alicia Curth, Valentyn Melnychuk, Stefan Feuerriegel, and Mihaela
 600 van der Schaar. A neural framework for generalized causal sensitivity analysis. In *ICLR*, 2024.

601

602 Andrew Jesson, Sören Mindermann, Yarin Gal, and Uri Shalit. Quantifying ignorance in individual-
 603 level causal-effect estimates under hidden confounding. In *ICML*, 2021.

604 Wenlong Ji, Lihua Lei, and Asher Spector. Model-agnostic covariate-assisted inference on partially
 605 identified causal effects. *arXiv preprint arXiv:2310.08115*, 2023.

606

607 Ying Jin, Zhimei Ren, and Emmanuel J. Candès. Sensitivity analysis of individual treatment effects:
 608 A robust conformal inference approach. *Proceedings of the National Academy of Sciences (PNAS)*,
 609 120(6), 2023.

610 Nathan Kallus. What's the harm? sharp bounds on the fraction negatively affected by treatment. In
 611 *NeurIPS*, 2022.

612

613 Nathan Kallus. Treatment effect risk: Bounds and inference. *Management Science*, 69(8):4579–4590,
 614 2023.

615 Nathan Kallus and Angela Zhou. Fairness, welfare, and equity in personalized pricing. In *FAccT*,
 616 2021.

617

618 Nathan Kallus, Xiaojie Mao, Kaiwen Wang, and Zhengyuan Zhou. Doubly robust distributionally
 619 robust off-policy evaluation and learning. In *ICML*, 2022.

620 Edward H. Kennedy. Semiparametric doubly robust targeted double machine learning: A review.
 621 *arXiv preprint*, 2022.

622

623 Edward H. Kennedy. Towards optimal doubly robust estimation of heterogeneous causal effects.
 624 *Electronic Journal of Statistics*, 17(2):3008–3049, 2023.

625

626 Edward H. Kennedy, Sivaraman Balakrishnan, and Larry Wasserman. Semiparametric counterfactual
 627 density estimation. *Biometrika*, 2023. ISSN 0006-3444.

628

629 Niki Kilbertus, Matt J. Kusner, and Ricardo Silva. A class of algorithms for general instrumental
 630 variable models. In *NeurIPS*, 2020.

631

632 Toru Kitagawa and Aleksey Tetenov. Who should be treated? empirical welfare maximization
 633 methods for treatment choice. *Econometrica*, 86(2):591–616, 2018.

634

635 Sungwon Lee. Partial identification and inference for conditional distributions of treatment effects.
 636 *Journal of Applied Econometrics*, 39(1):107–127, 2024.

637

638 Lihua Lei and Emmanuel J Candès. Conformal inference of counterfactuals and individual treatment
 639 effects. *Journal of the Royal Statistical Society Series B: Statistical Methodology*, 83(5):911–938,
 640 2021.

641

642 OV Lepskii. Asymptotically minimax adaptive estimation. i: Upper bounds. optimally adaptive
 643 estimates. *Theory of Probability & Its Applications*, 36(4):682–697, 1992.

644

645 OV Lepskii. Asymptotically minimax adaptive estimation. ii. schemes without optimal adaptation:
 646 Adaptive estimators. *Theory of Probability & Its Applications*, 37(3):433–448, 1993.

647

648 Alexander W Levis, Matteo Bonvini, Zhenghao Zeng, Luke Keele, and Edward H Kennedy. Covariate-
 649 assisted bounds on causal effects with instrumental variables. *Journal of the Royal Statistical
 650 Society Series B: Statistical Methodology*, pp. qkaf028, 2025.

651

652 Wei Liang and Changbao Wu. Estimation of treatment harm rate via partitioning. *arXiv preprint
 653 arXiv:2505.12209*, 2025.

648 Christos Louizos, Uri Shalit, Joris Mooij, David Sontag, Richard Zemel, and Max Welling. Causal
 649 effect inference with deep latent-variable models. In *NeurIPS*, 2017.
 650

651 Alexander R Luedtke and Mark J Van Der Laan. Statistical inference for the mean outcome under a
 652 possibly non-unique optimal treatment strategy. *Annals of statistics*, 44(2):713, 2016.
 653

654 GD Makarov. Estimates for the distribution function of a sum of two random variables when the
 655 marginal distributions are fixed. *Theory of Probability & its Applications*, 26(4):803–806, 1982.
 656

657 Charles F. Manski. Nonparametric bounds on treatment effects. *The American Economic Review*, 80
 658 (2):319–323, 1990.
 659

660 Valentyn Melnychuk, Stefan Feuerriegel, and Mihaela van der Schaar. Quantifying aleatoric uncer-
 661 tainty of the treatment effect: A novel orthogonal learner. In *NeurIPS*, 2024.
 662

663 Kirtan Padh, Jakob Zeitler, David Watson, Matt Kusner, Ricardo Silva, and Niki Kilbertus. Stochastic
 664 causal programming for bounding treatment effects. In *CLeR*, 2023.
 665

666 Gyungbae Park. Debiased machine learning when nuisance parameters appear in indicator functions.
 667 *arXiv preprint arXiv:2403.15934*, 2024.
 668

669 Richard AJ Post and Edwin R Van Den Heuvel. Beyond conditional averages: Estimating the
 670 individual causal effect distribution. *Journal of Causal Inference*, 13(1):20240007, 2025.
 671

672 James M. Robins. A new approach to causal inference in mortality studies with a sustained exposure
 673 period: Application to control of the healthy worker survivor effect. *Mathematical Modelling*, 7:
 674 1393–1512, 1986.
 675

676 James M. Robins, Andrea Rotnitzky, and Lue Ping Zhao. Estimation of reversion coefficients when
 677 some regressors are not always observed. *Journal of the American Statistical Association*, 89(427):
 678 846–888, 1994.
 679

680 Donald B. Rubin. Estimating causal effects of treatments in randomized and nonrandomized studies.
 681 *Journal of Educational Psychology*, 66(5):688–701, 1974. ISSN 0022-0663.
 682

683 Gabriel Ruiz and Oscar Hernan Madrid Padilla. High confidence inference on the probability an
 684 individual benefits from treatment using experimental or observational data with known propensity
 685 scores. *arXiv preprint arXiv:2205.09094*, 2022.
 686

687 Maresa Schröder, Dennis Frauen, Jonas Schweisthal, Konstantin Heß, Valentyn Melnychuk, and
 688 Stefan Feuerriegel. Conformal prediction for causal effects of continuous treatments. *arXiv
 689 preprint*, arXiv:2407.03094, 2024.
 690

691 Vira Semenova. Aggregated intersection bounds and aggregated minimax values. *arXiv preprint
 692 arXiv:2303.00982*, 2025.
 693

694 Uri Shalit, Fredrik D. Johansson, and David Sontag. Estimating individual treatment effect: General-
 695 ization bounds and algorithms. In *ICML*, 2017.
 696

697 Adith Swaminathan and Thorsten Joachims. Counterfactual risk minimization: Learning from logged
 698 bandit feedback. In *ICML*, 2015.
 699

700 Zhiqiang Tan. A distributional approach for causal inference using propensity scores. *Journal of the
 701 American Statistical Association*, 101(476):1619–1637, 2006.
 702

703 Mark J. van der Laan and Susan Gruber. Targeted minimum loss based estimation of causal effects of
 704 multiple time point interventions. *The International Journal of Biostatistics*, 8(1), 2012.
 705

706 Mark J. van der Laan and Donald B. Rubin. Targeted maximum likelihood learning. *The International
 707 Journal of Biostatistics*, 2(1), 2006.
 708

709 Aad W Van Der Vaart and Jon A Wellner. Weak convergence. In *Weak convergence and empirical
 710 processes: with applications to statistics*, pp. 16–28. Springer, 1996.
 711

702 Aart van der Vaart. *Asymptotic statistics*. Cambridge University Press, Cambridge, 1998. ISBN
703 0521496039.
704

705 Hal R. Varian. Causal inference in economics and marketing. *Proceedings of the National Academy*
706 *of Sciences (PNAS)*, 113(27):7310–7315, 2016.
707

708 Mingzhang Yin, Claudia Shi, Yixin Wang, and David M. Blei. Conformal sensitivity analysis for
709 individual treatment effects. *Journal of the American Statistical Association*, pp. 1–14, 2022.
710

711 Zhehao Zhang and Thomas S Richardson. Individual treatment effect: Prediction intervals and sharp
712 bounds. *arXiv preprint arXiv:2506.07469*, 2025.
713
714
715
716
717
718
719
720
721
722
723
724
725
726
727
728
729
730
731
732
733
734
735
736
737
738
739
740
741
742
743
744
745
746
747
748
749
750
751
752
753
754
755

756 A PROOFS.
757758 A.1 PROOF OF LEMMA 4.1
759760 *Proof.* Recall that the LSE operator is defined as

761
$$762 g_{t_1}(f) = \frac{1}{t_1} \log \left(\int \exp(t_1 f(y)) dy \right) \quad (23)$$

763

764 and that softplus function is defined as

765
$$766 h_{t_2}(u) = \frac{1}{t_2} \log(1 + e^{t_2 u}). \quad (24)$$

767

768 We can now write the smoothed Makarov bounds as
769

770
$$\rho_{t_1, t_2}^-(\delta) = \mathbb{E} \left[\frac{1}{t_2} \log \left(1 + I_{t_1, \delta}(X)^{\frac{t_2}{t_1}} \right) \right] = \mathbb{E} [h_{t_2}(g_{t_1}(F_1(\cdot|X) - F_0(\cdot - \delta|X)))] \quad (25)$$

771

772 and
773

774
$$\rho_{t_1, t_2}^+(\delta) = 1 - \mathbb{E} \left[\frac{1}{t_2} \log \left(1 + I_{-t_1, \delta}(X)^{\frac{t_2}{t_1}} \right) \right] = 1 + \mathbb{E} [h_{-t_2}(g_{-t_1}(F_1(\cdot|X) - F_0(\cdot - \delta|X)))]. \quad (26)$$

775
776

777 We now employ standard bounds on the softmax and LSE functions. For all $u \in \mathbb{R}$, $t_2 > 0$, it holds
778 that

779
$$h_{t_2}(u) - \frac{\log 2}{t_2} \leq (u)_+ \text{ and } (u)_- \leq h_{-t_2}(u) + \frac{\log 2}{t_2}. \quad (27)$$

780

781 For bounded $f : \mathcal{Y} \rightarrow \mathbb{R}$ on compact \mathcal{Y} and $t_1 > 0$, it holds that

782
$$783 g_{t_1}(f) - \frac{\log |\mathcal{Y}|}{t_1} \leq \sup_{y \in \mathcal{Y}} f(y) \text{ and } \inf_{y \in \mathcal{Y}} f(y) \leq g_{-t_1}(f) + \frac{\log |\mathcal{Y}|}{t_1}. \quad (28)$$

784

785 In the following, we prove the theorem for the lower Makarov bound but the argument for the upper
786 bound follows analogously. We apply the inequalities in (27) and (28) to Eq. (25) and obtain
787

788
$$\rho_{t_1, t_2}^-(\delta) \stackrel{(*)}{\leq} \mathbb{E} \left[h_{t_2} \left(\sup_{y \in \mathcal{Y}} (F_1(y|X) - F_0(y - \delta|X)) + \frac{\log |\mathcal{Y}|}{t_1} \right) \right] \quad (29)$$

789

790
$$\leq \mathbb{E} \left[\left(\sup_{y \in \mathcal{Y}} (F_1(y|X) - F_0(y - \delta|X)) + \frac{\log |\mathcal{Y}|}{t_1} \right)_+ \right] + \frac{\log 2}{t_2} \quad (30)$$

791

792
$$\stackrel{(**)}{\leq} \rho^-(\delta) + \frac{\log |\mathcal{Y}|_+}{t_1} + \frac{\log 2}{t_2}, \quad (31)$$

793

794 where (*) follows from monotonicity of h_{t_2} and (**) follows from $(a + b)_+ \leq a_+ + b_+$. \square
795796 A.2 PROOF OF THEOREM 4.2
797798 *Proof.* We start by deriving the efficient influence functions (EIFs) of the component $I_{t_1, \delta}(x)$. By
799 employing the chain rule for influence functions (Kennedy et al., 2023), we obtain
800

801
$$802 EIF\{I_{t_1, \delta}(x)\} = t_1 \int_{\mathcal{Y}} \exp(t_1 [F_1(y|x) - F_0(y - \delta|x)]) EIF\{F_1(y|x) - F_0(y - \delta|x)\} dy. \quad (32)$$

803

804 Hence, it holds that
805

806
$$EIF\{I_{t_1, \delta}(x)^{\frac{t_2}{t_1}}\} = \frac{t_2}{t_1} I_{t_1, \delta}(x)^{\frac{t_2}{t_1} - 1} EIF\{I_{t_1, \delta}(x)\} \quad (33)$$

807

808
$$809 = t_2 I_{t_1, \delta}(x)^{\frac{t_2}{t_1}} \int_{\mathcal{Y}} w_{t_1, \delta}(y|x) EIF\{F_1(y|x) - F_0(y - \delta|x)\} dy, \quad (34)$$

810 and for the upper bound analogue
 811

$$813 \quad EIF\{I_{-t_1,\delta}(x)^{\frac{t_2}{t_1}}\} = \frac{t_2}{t_1} I_{-t_1,\delta}(x)^{\frac{t_2}{t_1}-1} EIF\{I_{-t_1,\delta}(x)\} \quad (35)$$

$$814 \quad = -t_2 I_{-t_1,\delta}(x)^{\frac{t_2}{t_1}} \int_{\mathcal{Y}} w_{-t_1,\delta}(y|x) EIF\{F_1(y|x) - F_0(y-\delta|x)\} dy. \quad (36)$$

815
 816
 817
 818
 819
 820
 821 The efficient influence functions for the treatment and control c.d.f. are of standard form (Melnychuk
 822 et al., 2024), i.e.,
 823

$$824 \quad EIF\{F_a(y-\delta|X)\} = \frac{\mathbf{1}(A=a)\delta(X=x)}{\mathbb{P}(X=x, A=a)} (\mathbf{1}(Y \leq y-\delta) - F_a(y-\delta|x)). \quad (37)$$

825
 826
 827
 828
 829 Plugging everything together, the EIF for the lower smoothed Makarov bound is
 830

$$831 \quad \Psi_{t_1,t_2,\delta}^-(Z, \eta) \quad (38)$$

$$832 \quad = \int \frac{\mathbb{P}(X=x)}{t_2} EIF \log \left(1 + I_{t_1,\delta}(x)^{\frac{t_2}{t_1}} \right) dx \quad (39)$$

$$833 \quad + \frac{1}{t_2} \log \left(1 + I_{t_1,\delta}(X)^{\frac{t_2}{t_1}} \right) - \rho_{t_1,t_2}^-(\delta) \quad (40)$$

$$834 \quad = \int \frac{\mathbb{P}(X=x)}{t_2} \frac{EIF I_{t_1,\delta}(x)^{\frac{t_2}{t_1}}}{1 + I_{t_1,\delta}(x)^{\frac{t_2}{t_1}}} dx + \frac{1}{t_2} \log \left(1 + I_{t_1,\delta}(X)^{\frac{t_2}{t_1}} \right) - \rho_{t_1,t_2}^-(\delta) \quad (41)$$

$$835 \quad = \int \Pr(X=x) \underbrace{\frac{I_{t_1,\delta}(x)^{\frac{t_2}{t_1}}}{1 + I_{t_1,\delta}(x)^{\frac{t_2}{t_1}}}}_{\sigma_{t_1,t_2,\delta}^-(x)} \left[\int_{\mathcal{Y}} w_{t_1,\delta}(y|x) EIF\{F_1 - F_0\} dy \right] dx \quad (42)$$

$$836 \quad + \frac{1}{t_2} \log \left(1 + I_{t_1,\delta}(X)^{\frac{t_2}{t_1}} \right) - \rho_{t_1,t_2}^-(\delta) \quad (43)$$

$$837 \quad = \int \Pr(X=x) \sigma_{t_1,t_2,\delta}^-(x) \left[\int_{\mathcal{Y}} w_{t_1,\delta}(y|x) \frac{A\delta(X=x)}{\mathbb{P}(X=x, A=1)} (\mathbf{1}(Y \leq y) - F_1(y|x)) dy \right] dx \quad (44)$$

$$838 \quad - \int \Pr(X=x) \sigma_{t_1,t_2,\delta}^-(x) \left[\int_{\mathcal{Y}} w_{t_1,\delta}(y|x) \frac{(1-A)\delta(X=x)}{\mathbb{P}(X=x, A=0)} (\mathbf{1}(Y \leq y-\delta) - F_0(y-\delta|x)) dy \right] dx \quad (45)$$

$$839 \quad + \frac{1}{t_2} \log \left(1 + I_{t_1,\delta}(X)^{\frac{t_2}{t_1}} \right) - \rho_{t_1,t_2}^-(\delta) \quad (46)$$

$$840 \quad = \sigma_{t_1,t_2,\delta}^-(X) \left[\int_{\mathcal{Y}} w_{t_1,\delta}(y|X) \frac{A}{\pi(X)} (\mathbf{1}(Y \leq y) - F_1(y|X)) dy \right] \quad (47)$$

$$841 \quad - \sigma_{t_1,t_2,\delta}^-(X) \left[\int_{\mathcal{Y}} w_{t_1}(y|X) \frac{(1-A)}{1-\pi(X)} (\mathbf{1}(Y \leq y-\delta) - F_0(y-\delta|X)) dy \right] \quad (48)$$

$$842 \quad + \frac{1}{t_2} \log \left(1 + I_{t_1,\delta}(X)^{\frac{t_2}{t_1}} \right) - \rho_{t_1,t_2}^-(\delta) \quad (49)$$

$$843 \quad (50)$$

Analogously, we obtain the EIF for the upper smoothed Makarov bound as

$$\Psi_{t_1, t_2, \delta}^+(Z, \eta) \quad (51)$$

$$= \int \mathbb{P}(X = x) EIF \left\{ 1 - \frac{1}{t_2} \log \left(1 + I_{-t_1, \delta}(x)^{\frac{t_2}{t_1}} \right) \right\} dx \quad (52)$$

$$+ 1 - \frac{1}{t_2} \log \left(1 + I_{-t_1, \delta}(X)^{\frac{t_2}{t_1}} \right) - \rho_{t_1, t_2}^+(\delta) \quad (53)$$

$$= \int \frac{\mathbb{P}(X = x)}{-t_2} EIF \log \left(1 + I_{-t_1, \delta}(x)^{\frac{t_2}{t_1}} \right) dx \quad (54)$$

$$+ 1 - \frac{1}{t_2} \log \left(1 + I_{-t_1, \delta}(X)^{\frac{t_2}{t_1}} \right) - \rho_{t_1, t_2}^+(\delta) \quad (55)$$

$$= \int \frac{\mathbb{P}(X = x)}{-t_2} \frac{EIF I_{-t_1, \delta}(x)^{\frac{t_2}{t_1}}}{1 + I_{-t_1, \delta}(x)^{\frac{t_2}{t_1}}} dx + 1 - \frac{1}{t_2} \log \left(1 + I_{-t_1, \delta}(X)^{\frac{t_2}{t_1}} \right) - \rho_{t_1, t_2}^+(\delta) \quad (56)$$

$$= \int \Pr(X = x) \underbrace{\frac{I_{-t_1, \delta}(x)^{\frac{t_2}{t_1}}}{1 + I_{-t_1, \delta}(x)^{\frac{t_2}{t_1}}}}_{\sigma_{t_1, t_2, \delta}^+(x)} \left[\int_{\mathcal{Y}} w_{-t_1, \delta}(y|x) EIF\{F_1 - F_0\} dy \right] dx \quad (57)$$

$$+ 1 - \frac{1}{t_2} \log \left(1 + I_{-t_1, \delta}(X)^{\frac{t_2}{t_1}} \right) - \rho_{t_1, t_2}^+(\delta) \quad (58)$$

$$= \int \Pr(X = x) \sigma_{t_1, t_2, \delta}^+(x) \left[\int_{\mathcal{Y}} w_{-t_1, \delta}(y|x) \frac{A\delta(X = x)}{\mathbb{P}(X = x, A = 1)} (\mathbf{1}(Y \leq y) - F_1(y|x)) dy \right] dx \quad (59)$$

$$- \int \Pr(X = x) \sigma_{t_1, t_2, \delta}^+(x) \left[\int_{\mathcal{Y}} w_{-t_1, \delta}(y|x) \frac{(1 - A)\delta(X = x)}{\mathbb{P}(X = x, A = 0)} (\mathbf{1}(Y \leq y - \delta) - F_0(y - \delta|x)) dy \right] dx \quad (60)$$

$$+ 1 - \frac{1}{t_2} \log \left(1 + I_{-t_1, \delta}(X)^{\frac{t_2}{t_1}} \right) - \rho_{t_1, t_2}^+(\delta) \quad (61)$$

$$= \sigma_{t_1, t_2, \delta}^+(X) \left[\int_{\mathcal{Y}} w_{-t_1, \delta}(y|X) \frac{A}{\pi(X)} (\mathbf{1}(Y \leq y) - F_1(y|X)) dy \right] \quad (62)$$

$$- \sigma_{t_1, t_2, \delta}^+(X) \left[\int_{\mathcal{Y}} w_{-t_1, \delta}(y|X) \frac{(1 - A)}{1 - \pi(X)} (\mathbf{1}(Y \leq y - \delta) - F_0(y - \delta|X)) dy \right] \quad (63)$$

$$+ 1 - \frac{1}{t_2} \log \left(1 + I_{-t_1, \delta}(X)^{\frac{t_2}{t_1}} \right) - \rho_{t_1, t_2}^+(\delta). \quad (64)$$

□

A.3 PROOF OF COROLLARY 4.3

Assumption A.1 (Regularity and rate conditions for Corollary 4.3). Fix $\delta \in \mathbb{R}$ and smoothing parameters $t_1, t_2 > 0$. Let $Z = (X, A, Y) \sim \mathbb{P}$ denote a generic observation and let $\eta = (F_0, F_1, \pi)$ denote the collection of nuisance functions.

1. **Causal assumptions.** Assumption 3.1 holds: consistency, overlap, and ignorability.

2. **Outcome support and boundedness.** The outcome support \mathcal{Y} is compact with finite Lebesgue measure, as in Lemma 4.1. The efficient influence functions $\Psi_{t_1, t_2, \delta}^{\pm}(Z, \eta, \theta^{\pm}(\delta))$ in Theorem 4.2 are square-integrable with strictly positive and finite variance

$$0 < V^{\pm}(\delta) := \text{Var}(\Psi_{t_1, t_2, \delta}^{\pm}(Z, \eta, \theta^{\pm}(\delta))) < \infty.$$

3. **Cross-fitting.** The estimators $\hat{\eta} = (\hat{F}_0, \hat{F}_1, \hat{\pi})$ are obtained with sample splitting / K -fold cross-fitting: for each observation i , the corresponding nuisance estimates $\hat{\eta}^{(-k(i))}$ are trained on all folds except the one containing i .

918 4. **Rate conditions for nuisances.** For $a \in \{0, 1\}$,

919

$$920 \|\hat{F}_a - F_a\|_2 = o_{\mathbb{P}}(n^{-1/4}), \quad \|\hat{\pi} - \pi\|_2 = o_{\mathbb{P}}(n^{-1/4}),$$

921

922 where $\|\cdot\|_2$ denotes the $L_2(\mathbb{P})$ norm.

923

924 *Proof of Corollary 4.3.* Fix $\delta \in \mathbb{R}$ and abbreviate

925

926

$$\theta^{\pm}(\delta) = \rho_{t_1, t_2}^{\pm}(\delta), \quad \hat{\theta}^{\pm}(\delta) = \hat{\rho}_{t_1, t_2}^{\pm}(\delta),$$

927

928 for the smoothed lower and upper Makarov bounds and their debiased estimators in (19). For
929 readability we suppress the dependence on δ where no confusion arises.
930

931 **Step 1: Oracle influence function representation.** By Theorem 4.2 and Assumption A.1(v),
932 the smoothed functionals θ^{\pm} are pathwise differentiable at \mathbb{P} with efficient influence functions
933 $\Psi_{t_1, t_2, \delta}^{\pm}(Z, \eta, \theta^{\pm}(\delta))$. Consider the oracle estimator
934

935

$$\tilde{\theta}^{\pm}(\delta) := \frac{1}{n} \sum_{i=1}^n \left(\theta^{\pm}(\delta) + \Psi_{t_1, t_2, \delta}^{\pm}(Z_i, \eta, \theta^{\pm}(\delta)) \right),$$

936

937 which satisfies

938

939

$$\tilde{\theta}^{\pm}(\delta) - \theta^{\pm}(\delta) = \frac{1}{n} \sum_{i=1}^n \Psi_{t_1, t_2, \delta}^{\pm}(Z_i, \eta, \theta^{\pm}(\delta)).$$

940

941 By Assumption A.1(ii), the summands are i.i.d. with mean zero and variance $V^{\pm}(\delta) \in (0, \infty)$, so
942 the Lindeberg–Feller central limit theorem yields
943

944

$$\sqrt{n}(\tilde{\theta}^{\pm}(\delta) - \theta^{\pm}(\delta)) \Rightarrow \mathcal{N}(0, V^{\pm}(\delta)). \quad (65)$$

945

946 **Step 2: Effect of plug-in nuisance estimation with cross-fitting.** Let the sample be partitioned
947 into K folds and denote by $\hat{\eta}^{(-k)}$ the nuisance estimates trained on all folds except fold k . For each
948 i , let $k(i)$ be the index of the fold containing Z_i . The debiased estimators with cross-fitting can be
949 written as
950

951

$$\hat{\theta}^{\pm}(\delta) = \frac{1}{n} \sum_{i=1}^n \left(\theta^{\pm}(\delta) + \Psi_{t_1, t_2, \delta}^{\pm}(Z_i, \hat{\eta}^{(-k(i))}, \theta^{\pm}(\delta)) \right) + R_n^{\pm},$$

952

953 where R_n^{\pm} collects the higher-order terms arising from replacing $\theta^{\pm}(\delta)$ by $\hat{\theta}^{\pm}(\delta)$ inside the influence
954 function.
955

956 By Neyman orthogonality of the score in Theorem 4.2 and Assumption A.1(iii)–(iv), standard
957 arguments for orthogonal / debiased estimation (see, e.g., Chernozhukov et al. (2018)) imply that
958

959

$$\left| \frac{1}{n} \sum_{i=1}^n \left(\Psi_{t_1, t_2, \delta}^{\pm}(Z_i, \hat{\eta}^{(-k(i))}, \theta^{\pm}(\delta)) - \Psi_{t_1, t_2, \delta}^{\pm}(Z_i, \eta, \theta^{\pm}(\delta)) \right) \right| = o_{\mathbb{P}}(n^{-1/2}),$$

960

961 and that $R_n^{\pm} = o_{\mathbb{P}}(n^{-1/2})$ by a Taylor expansion in θ . Hence we obtain the linear expansion
962

963

$$\hat{\theta}^{\pm}(\delta) - \theta^{\pm}(\delta) = \frac{1}{n} \sum_{i=1}^n \Psi_{t_1, t_2, \delta}^{\pm}(Z_i, \eta, \theta^{\pm}(\delta)) + r_n^{\pm}, \quad r_n^{\pm} = o_{\mathbb{P}}(n^{-1/2}). \quad (66)$$

964

965 Comparing (66) with the oracle representation shows that the leading term is identical and the
966 remainder is negligible at the \sqrt{n} scale. Combining (65) and (66) and applying Slutsky’s lemma
967 gives, for each fixed δ ,

968

969

$$\sqrt{n}(\hat{\theta}^{\pm}(\delta) - \theta^{\pm}(\delta)) \Rightarrow \mathcal{N}(0, V^{\pm}(\delta)). \quad (67)$$

970

972 **Step 3: Consistency of the standard error estimator.** Define
 973

$$974 \quad \widehat{V}^{\pm}(\delta) = \frac{1}{n} \sum_{i=1}^n \left(\Psi_{t_1, t_2, \delta}^{\pm}(Z_i, \hat{\eta}^{(-k(i))}, \hat{\theta}^{\pm}(\delta)) - \bar{\Psi}^{\pm}(\delta) \right)^2,$$

$$975$$

$$976$$

977 where

$$978 \quad \bar{\Psi}^{\pm}(\delta) = \frac{1}{n} \sum_{i=1}^n \Psi_{t_1, t_2, \delta}^{\pm}(Z_i, \hat{\eta}^{(-k(i))}, \hat{\theta}^{\pm}(\delta)),$$

$$979$$

$$980$$

981 and set $\widehat{\text{se}}^{\pm}(\delta) = \sqrt{\widehat{V}^{\pm}(\delta)/n}$.

982 By the same orthogonality and rate conditions as in Step 2, the difference between
 983

$$984 \quad \Psi_{t_1, t_2, \delta}^{\pm}(Z_i, \hat{\eta}^{(-k(i))}, \hat{\theta}^{\pm}(\delta)) \quad \text{and} \quad \Psi_{t_1, t_2, \delta}^{\pm}(Z_i, \eta, \theta^{\pm}(\delta))$$

$$985$$

986 is $o_{\mathbb{P}}(1)$ in L_2 uniformly in i . A law of large numbers under cross-fitting then yields

$$987 \quad \widehat{V}^{\pm}(\delta) \xrightarrow{\mathbb{P}} V^{\pm}(\delta),$$

$$988$$

989 so $\widehat{\text{se}}^{\pm}(\delta) \xrightarrow{\mathbb{P}} \sqrt{V^{\pm}(\delta)/n}$. Combining this with (67) and using Slutsky's lemma again, we obtain
 990 the studentized central limit theorem
 991

$$992 \quad \frac{\hat{\theta}^{\pm}(\delta) - \theta^{\pm}(\delta)}{\widehat{\text{se}}^{\pm}(\delta)} \Rightarrow \mathcal{N}(0, 1). \quad (68)$$

$$993$$

$$994$$

995 **Step 4: One-sided intervals for the smoothed bounds.** From (68), for each fixed δ ,
 996

$$997 \quad \Pr \left\{ \theta^-(\delta) \geq \hat{\theta}^-(\delta) - z_{1-\alpha/2} \widehat{\text{se}}^-(\delta) \right\} \rightarrow 1 - \alpha/2,$$

$$998$$

999 and

$$1000 \quad \Pr \left\{ \theta^+(\delta) \leq \hat{\theta}^+(\delta) + z_{1-\alpha/2} \widehat{\text{se}}^+(\delta) \right\} \rightarrow 1 - \alpha/2,$$

$$1001$$

1002 where $z_{1-\alpha/2}$ is the $(1 - \alpha/2)$ quantile of the standard normal distribution.
 1003

1003 **Step 5: Translating to the original Makarov bounds.** By Lemma 4.1, for all fixed $t_1, t_2 > 0$,
 1004

$$1005 \quad \theta^-(\delta) - b(t_1, t_2) \leq \rho(\delta) \leq \theta^+(\delta) + b(t_1, t_2),$$

$$1006$$

1006 where $b(t_1, t_2)$ is the approximation bias bound. On the intersection of the two one-sided events from
 1007 Step 4, we have

$$1008 \quad \hat{\theta}^-(\delta) - z_{1-\alpha/2} \widehat{\text{se}}^-(\delta) - b(t_1, t_2) \leq \rho(\delta) \leq \hat{\theta}^+(\delta) + z_{1-\alpha/2} \widehat{\text{se}}^+(\delta) + b(t_1, t_2).$$

$$1009$$

1010 By the definition of $c_{t_1, t_2, \delta, \alpha}^-(\mathcal{D}_n)$ and $c_{t_1, t_2, \delta, \alpha}^+(\mathcal{D}_n)$, this event is precisely
 1011

$$1012 \quad c_{t_1, t_2, \delta, \alpha}^-(\mathcal{D}_n) \leq \rho(\delta) \leq c_{t_1, t_2, \delta, \alpha}^+(\mathcal{D}_n).$$

$$1013$$

1014 A Bonferroni argument then yields

$$1015 \quad \lim_{n \rightarrow \infty} \Pr \left\{ c_{t_1, t_2, \delta, \alpha}^-(\mathcal{D}_n) \leq \rho(\delta) \leq c_{t_1, t_2, \delta, \alpha}^+(\mathcal{D}_n) \right\} \geq 1 - \alpha,$$

$$1016$$

1017 which proves the corollary. \square
 1018

1019
 1020
 1021
 1022
 1023
 1024
 1025

1026 **B EXTENDED RELATED WORK**
10271028 **Semiparametric efficient causal inference.** Semiparametric efficiency theory (van der Vaart, 1998)
1029 and efficient-influence function-based estimators have a long tradition in causal inference (Kennedy,
1030 2022). Examples include the AIPTW estimator (Robins et al., 1994), Targeted maximum-likelihood
1031 estimation (TMLE) (van der Laan & Rubin, 2006). These frameworks have been extended to various
1032 causal quantities and are the de-facto standard for modern causal effect estimation in many settings
1033 (van der Laan & Gruber, 2012; Chernozhukov et al., 2018; Foster & Syrgkanis, 2023; Kennedy,
1034 2023).1035 **Bounds for partially identified causal quantities** In many situations, the causal parameter of interest
1036 is only *partially* identified. That is, we need to obtain bounds on the parameter of interest which we
1037 can then estimate with observational data Manski (1990). Several works have proposed methods
1038 for partial identification of causal quantities, including treatment effects in instrumental variable
1039 settings Balke & Pearl (1997); Kilbertus et al. (2020) and more general causal graphs Duarte et al.
1040 (2023); Balazadeh et al. (2022); Chen et al. (2023); Padh et al. (2023), and treatment effect risk
1041 Kallus (2023). A related stream of literature obtains bounds under so-called sensitivity models, which
1042 impose assumptions on the degree of non-identifiability Tan (2006); Jesson et al. (2021); Dorn &
1043 Guo (2022); Dorn et al. (2024); Yin et al. (2022); Frauen et al. (2023); Jin et al. (2023); Frauen et al.
1044 (2024).1045
1046
1047
1048
1049
1050
1051
1052
1053
1054
1055
1056
1057
1058
1059
1060
1061
1062
1063
1064
1065
1066
1067
1068
1069
1070
1071
1072
1073
1074
1075
1076
1077
1078
1079

1080 C EXTENSION TO DISCRETE OUTCOMES.
1081

1082 Here we provide minimal changes needed to extend our methodology to discrete outcomes. Let
1083 $\mathcal{Y}_d = \{y_1 < \dots < y_M\}$ denote a finite ordered support. For $a \in \{0, 1\}$, write $F_a(\cdot | x)$ for the
1084 right-continuous conditional CDF of $Y | (A = a, X = x)$ on \mathcal{Y}_d . All other notation is as in the main
1085 text.

1086 **Discrete log-sum-exp and softplus.** The softplus $h_{t_2}(u) = t_2^{-1} \log(1 + e^{t_2 u})$ is unchanged. We
1087 replace the continuous log-sum-exp with its discrete analogue
1088

$$1090 \quad 1091 \quad 1092 \quad g_{t_1}^{(d)}(f) = \frac{1}{t_1} \log \left(\sum_{y \in \mathcal{Y}_d} \exp\{t_1 f(y)\} \right). \quad (69)$$

1093 Accordingly, define the discrete normalizer
1094

$$1095 \quad 1096 \quad 1097 \quad I_{t,\delta}^{(d)}(x) = \sum_{y \in \mathcal{Y}_d} \exp\left(t[F_1(y | x) - F_0(y - \delta | x)]\right). \quad (70)$$

1098 **Smoothed Makarov bounds (discrete).** Replacing the operators in Sec. 4.1 by (69)–(70) yields
1099 the discrete smoothed bounds
1100

$$1101 \quad 1102 \quad 1103 \quad \rho_{t_1,t_2}^{-(d)}(\delta) = \mathbb{E}\left[\frac{1}{t_2} \log\left(1 + (I_{t_1,\delta}^{(d)}(X))^{t_2/t_1}\right)\right], \quad \rho_{t_1,t_2}^{+(d)}(\delta) = 1 - \mathbb{E}\left[\frac{1}{t_2} \log\left(1 + (I_{-t_1,\delta}^{(d)}(X))^{t_2/t_1}\right)\right]. \quad (71)$$

1104 The analogue of Lemma 4.1 holds with the discrete approximation bias

$$1105 \quad 1106 \quad 1107 \quad b_d(t_1, t_2) = \frac{\log 2}{t_2} + \frac{\log M}{t_1}, \quad (72)$$

1108 i.e. $\rho_{t_1,t_2}^{-(d)}(\delta) - b_d(t_1, t_2) \leq \rho^-(\delta)$ and $\rho^+(\delta) \leq \rho_{t_1,t_2}^{+(d)}(\delta) + b_d(t_1, t_2)$, with $\rho_{t_1,t_2}^{\pm,d}(\delta) \rightarrow \rho^{\pm}(\delta)$ as
1109 $t_1, t_2 \rightarrow \infty$.

1111 **Efficient influence functions (discrete).** The EIFs in Theorem 4.2 carry over after replacing all
1112 integrals over y by sums over \mathcal{Y}_d . Define the discrete softmax weights
1113

$$1114 \quad 1115 \quad 1116 \quad w_{t_1,\delta}^{(d)}(y | x) = \frac{\exp\left(t_1[F_1(y | x) - F_0(y - \delta | x)]\right)}{I_{t_1,\delta}^{(d)}(x)}, \quad y \in \mathcal{Y}_d, \quad (73)$$

1118 and the discrete analogue of $\Phi_{t_1,\delta}^a$,

$$1120 \quad 1121 \quad 1122 \quad \Phi_{t_1,\delta}^{a,(d)}(X, Y) = \sum_{y \in \mathcal{Y}_d} w_{t_1,\delta}^{(d)}(y | X) \left(\mathbf{1}\{Y \leq y - (1-a)\delta\} - F_a(y - (1-a)\delta | X) \right). \quad (74)$$

1123 With $\sigma_{t_1,t_2,\delta}^{\pm}(x)$ defined exactly as in the main text but using $I_{\pm t_1,\delta}^{(d)}(x)$, the EIFs are
1124

$$1125 \quad 1126 \quad 1127 \quad \Psi_{t_1,t_2,\delta}^{-(d)}(Z, \eta, \rho_{t_1,t_2}^{-(d)}(\delta)) = \sigma_{t_1,t_2,\delta}^-(X) \left[\frac{A}{\pi(X)} \Phi_{t_1,\delta}^{1,(d)}(X, Y) - \frac{1-A}{1-\pi(X)} \Phi_{t_1,\delta}^{0,(d)}(X, Y) \right] \\ 1128 \quad + \frac{1}{t_2} \log\left(1 + (I_{t_1,\delta}^{(d)}(X))^{t_2/t_1}\right) - \rho_{t_1,t_2}^{-(d)}(\delta). \quad (75)$$

$$1131 \quad 1132 \quad 1133 \quad \Psi_{t_1,t_2,\delta}^{+(d)}(Z, \eta, \rho_{t_1,t_2}^{+(d)}(\delta)) = \sigma_{t_1,t_2,\delta}^+(X) \left[\frac{A}{\pi(X)} \Phi_{-t_1,\delta}^{1,(d)}(X, Y) - \frac{1-A}{1-\pi(X)} \Phi_{-t_1,\delta}^{0,(d)}(X, Y) \right] \\ 1134 \quad + 1 - \frac{1}{t_2} \log\left(1 + (I_{-t_1,\delta}^{(d)}(X))^{t_2/t_1}\right) - \rho_{t_1,t_2}^{+(d)}(\delta). \quad (76)$$

1134 **Debiased estimators (discrete).** The one-step estimators in Eq. (19) become
 1135

$$1136 \hat{\rho}_{t_1, t_2}^{-(d)}(\delta) = \frac{1}{n} \sum_{i=1}^n \left\{ \frac{1}{t_2} \log \left(1 + (\hat{I}_{t_1, \delta}^{(d)}(x_i))^{t_2/t_1} \right) + \hat{\sigma}_{t_1, t_2, \delta}^-(x_i) \frac{a_i - \hat{\pi}(x_i)}{\hat{\pi}(x_i)\{1 - \hat{\pi}(x_i)\}} \hat{\Phi}_{t_1, \delta}^{a_i, (d)}(x_i, y_i) \right\}. \quad (77)$$

$$1139 \hat{\rho}_{t_1, t_2}^{+(d)}(\delta) = \frac{1}{n} \sum_{i=1}^n \left\{ 1 - \frac{1}{t_2} \log \left(1 + (\hat{I}_{-t_1, \delta}^{(d)}(x_i))^{t_2/t_1} \right) + \hat{\sigma}_{t_1, t_2, \delta}^+(x_i) \frac{a_i - \hat{\pi}(x_i)}{\hat{\pi}(x_i)\{1 - \hat{\pi}(x_i)\}} \hat{\Phi}_{-t_1, \delta}^{a_i, (d)}(x_i, y_i) \right\}. \quad (78)$$

1142 Here $\hat{I}_{\pm t_1, \delta}^{(d)}$, $\hat{w}_{t_1, \delta}^{(d)}$, and $\hat{\Phi}_{\pm t_1, \delta}^{a_i, (d)}$ replace (70), (73), and (74) with estimated nuisances. Cross-fitting
 1143 and variance estimation via the sample variance of the estimated EIF proceed unchanged.
 1144

1145
 1146
 1147
 1148
 1149
 1150
 1151
 1152
 1153
 1154
 1155
 1156
 1157
 1158
 1159
 1160
 1161
 1162
 1163
 1164
 1165
 1166
 1167
 1168
 1169
 1170
 1171
 1172
 1173
 1174
 1175
 1176
 1177
 1178
 1179
 1180
 1181
 1182
 1183
 1184
 1185
 1186
 1187

1188 **D EXTENSION TO UNIFORMLY VALID CONFIDENCE INTERVALS**
 1189

1190 In this section, we extend Corollary 4.3 to construct confidence intervals for the treatment effect
 1191 distribution that are *simultaneously* valid for all values of δ in a compact set $\Delta \subset \mathbb{R}$. The construction
 1192 proceeds in two steps. First, we establish a functional central limit theorem (CLT) for the smoothed
 1193 debiased estimators $\hat{\rho}_{t_1, t_2}^\pm(\delta)$ viewed as stochastic processes in δ . Second, we use a multiplier
 1194 bootstrap to approximate the distribution of the supremum of the corresponding Gaussian limit
 1195 and combine this with the approximation bias bound $b(t_1, t_2)$ from Lemma 4.1 to obtain uniform
 1196 confidence bands for the original Makarov bounds.

1197 **D.1 UNIFORM ASYMPTOTIC LINEARITY AND FUNCTIONAL CLT**
 1198

1199 We focus on a compact interval $\Delta \subset \mathbb{R}$ of values of δ that are of substantive interest. Throughout this
 1200 section, we treat the smoothing parameters (t_1, t_2) as fixed and suppress their dependence where it is
 1201 notationally convenient. We write

$$1203 \mathbb{G}_n f = \frac{1}{\sqrt{n}} \sum_{i=1}^n (f(Z_i) - \mathbb{E}[f(Z)])$$

1204 for the empirical process indexed by a function f , and consider the class of efficient influence
 1205 functions

$$1206 \mathcal{F}^\pm = \{\Psi_{t_1, t_2, \delta}^\pm(\cdot, \eta, \rho_{t_1, t_2}^\pm(\delta)) : \delta \in \Delta\}$$

1207 as given in Theorem 4.2.

1208 We impose the following regularity condition, which is a uniform version of the high-level conditions
 1209 used in Corollary 4.3.

1210 **Assumption D.1** (Uniform regularity of the EIF process). Let $\Delta \subset \mathbb{R}$ be compact and let
 1211 $\Psi_{t_1, t_2, \delta}^\pm(Z, \eta, \rho_{t_1, t_2}^\pm(\delta))$ be as in Theorem 4.2. Assume:

1212 **1. Uniform bounded second moments:**

$$1213 \sup_{\delta \in \Delta} \mathbb{E}[\Psi_{t_1, t_2, \delta}^\pm(Z, \eta, \rho_{t_1, t_2}^\pm(\delta))^2] < \infty.$$

1214 **2. Stochastic equicontinuity in δ :** there exists a semi-metric d on Δ such that, for any $\varepsilon > 0$,

$$1215 \lim_{\gamma \rightarrow 0} \limsup_{n \rightarrow \infty} \mathbb{P}\left(\sup_{d(\delta, \delta') \leq \gamma} |\mathbb{G}_n(\Psi_{t_1, t_2, \delta}^\pm - \Psi_{t_1, t_2, \delta'}^\pm)| > \varepsilon \right) = 0.$$

1216 **3. Donsker-type condition:** the class \mathcal{F}^\pm is P -Donsker (or, more generally, satisfies an
 1217 entropy condition that guarantees a functional CLT for \mathbb{G}_n indexed by \mathcal{F}^\pm).

1218 **4. Uniform orthogonality and nuisance rates:** let $\hat{\eta}$ be obtained via sample splitting as in
 1219 Corollary 4.3. The asymptotic linear expansion

$$1220 \hat{\rho}_{t_1, t_2}^\pm(\delta) = \rho_{t_1, t_2}^\pm(\delta) + \frac{1}{n} \sum_{i=1}^n \Psi_{t_1, t_2, \delta}^\pm(Z_i, \eta, \rho_{t_1, t_2}^\pm(\delta)) + r_n^\pm(\delta)$$

1221 holds with a remainder satisfying

$$1222 \sup_{\delta \in \Delta} \sqrt{n} |r_n^\pm(\delta)| \xrightarrow{P} 0.$$

1223 Under Assumption D.1, we obtain a functional CLT for the smoothed lower and upper bounds
 1224 following standard arguments in empirical process theory (Van Der Vaart & Wellner, 1996).

1225 **Theorem D.2** (Functional CLT for smoothed Makarov bounds). *Let Assumption D.1 hold and let
 1226 $\Delta \subset \mathbb{R}$ be compact. Then, in the space $\ell^\infty(\Delta)$ of bounded real-valued functions on Δ ,*

$$1227 \{\sqrt{n}(\hat{\rho}_{t_1, t_2}^-(\delta) - \rho_{t_1, t_2}^-(\delta))\}_{\delta \in \Delta} \rightsquigarrow \{G^-(\delta)\}_{\delta \in \Delta}, \quad (79)$$

$$1228 \{\sqrt{n}(\hat{\rho}_{t_1, t_2}^+(\delta) - \rho_{t_1, t_2}^+(\delta))\}_{\delta \in \Delta} \rightsquigarrow \{G^+(\delta)\}_{\delta \in \Delta}, \quad (80)$$

1242 where G^\pm are mean-zero tight Gaussian processes with covariance functions
 1243

$$1244 \text{Cov}(G^\pm(\delta_1), G^\pm(\delta_2)) = \mathbb{E}[\Psi_{t_1, t_2, \delta_1}^\pm(Z, \eta, \rho_{t_1, t_2}^\pm(\delta_1)) \Psi_{t_1, t_2, \delta_2}^\pm(Z, \eta, \rho_{t_1, t_2}^\pm(\delta_2))]$$

1245 for all $\delta_1, \delta_2 \in \Delta$.
 1246

1247 As a consequence of Theorem D.2, the random variables
 1248

$$1249 \sup_{\delta \in \Delta} |\sqrt{n}(\hat{\rho}_{t_1, t_2}^\pm(\delta) - \rho_{t_1, t_2}^\pm(\delta))|$$

1250 converge in distribution to $\sup_{\delta \in \Delta} |G^\pm(\delta)|$. We now describe how to approximate the distribution of
 1251 these suprema via a multiplier bootstrap.
 1252

1253 D.2 MULTIPLIER BOOTSTRAP FOR UNIFORM BANDS OF SMOOTHED BOUNDS

1255 Define the estimated influence function contributions
 1256

$$1257 \hat{\psi}_i^\pm(\delta) = \Psi_{t_1, t_2, \delta}^\pm(Z_i, \hat{\eta}, \hat{\rho}_{t_1, t_2}^\pm(\delta)), \quad i = 1, \dots, n, \quad \delta \in \Delta,$$

1258 where $\hat{\eta}$ and $\hat{\rho}_{t_1, t_2}^\pm(\delta)$ are obtained as in Eq. (19). Let
 1259

$$1260 \bar{\hat{\psi}}_n^\pm(\delta) = \frac{1}{n} \sum_{i=1}^n \hat{\psi}_i^\pm(\delta)$$

1263 denote the empirical mean of these contributions.
 1264

1265 Let ξ_1, \dots, ξ_n be i.i.d. multiplier weights with $\mathbb{E}[\xi_i] = 0$ and $\mathbb{E}[\xi_i^2] = 1$ (e.g., Rademacher or standard
 1266 normal). The multiplier bootstrap process is defined by

$$1267 \hat{G}_n^{\pm,*}(\delta) = \frac{1}{\sqrt{n}} \sum_{i=1}^n \xi_i (\hat{\psi}_i^\pm(\delta) - \bar{\hat{\psi}}_n^\pm(\delta)), \quad \delta \in \Delta. \quad (81)$$

1270 We then consider the sup-norm statistic
 1271

$$1272 T_n^{\pm,*} = \sup_{\delta \in \Delta} |\hat{G}_n^{\pm,*}(\delta)|.$$

1274 Repeating this construction B times with independent multipliers $\{\xi_i^{(b)}\}_{i=1}^n, b = 1, \dots, B$, yields
 1275 bootstrap draws
 1276

$$1277 T_{n,1}^{\pm,*}, \dots, T_{n,B}^{\pm,*}.$$

1278 Let $\hat{c}_{1-\alpha}^\pm$ denote the empirical $(1 - \alpha)$ quantile of $\{T_{n,b}^{\pm,*}\}_{b=1}^B$. Under standard conditions for
 1279 the validity of the multiplier bootstrap for suprema of empirical processes (which are implied by
 1280 Assumption D.1 and mild additional technical assumptions), this quantity consistently estimates the
 1281 $(1 - \alpha)$ quantile of $\sup_{\delta \in \Delta} |G^\pm(\delta)|$.

1282 The following corollary summarizes the resulting uniform confidence bands for the *smoothed* bounds
 1283 $\rho_{t_1, t_2}^\pm(\delta)$, following standard multiplier bootstrap theory for empirical processes (Van Der Vaart &
 1284 Wellner, 1996).

1285 **Corollary D.3** (Simultaneous confidence bands for smoothed Makarov bounds). *Suppose the conditions of Theorem D.2 hold and the multiplier bootstrap described in Eq. (81) is valid for the processes in (79)–(80). Let $\hat{c}_{1-\alpha}^\pm$ be the empirical $(1 - \alpha)$ quantiles of $T_n^{\pm,*}$ as defined above. Then,*

$$1289 \lim_{n \rightarrow \infty} \mathbb{P} \left(\forall \delta \in \Delta : |\hat{\rho}_{t_1, t_2}^\pm(\delta) - \rho_{t_1, t_2}^\pm(\delta)| \leq \frac{\hat{c}_{1-\alpha}^\pm}{\sqrt{n}} \right) \geq 1 - \alpha.$$

1292 Equivalently, the bands
 1293

$$1294 \delta \mapsto \left[\hat{\rho}_{t_1, t_2}^\pm(\delta) - \frac{\hat{c}_{1-\alpha}^\pm}{\sqrt{n}}, \hat{\rho}_{t_1, t_2}^\pm(\delta) + \frac{\hat{c}_{1-\alpha}^\pm}{\sqrt{n}} \right]$$

1295 are asymptotically valid $(1 - \alpha)$ simultaneous confidence bands for the smoothed Makarov bounds
 1296 $\rho_{t_1, t_2}^\pm(\delta)$, uniformly over $\delta \in \Delta$.

1296 D.3 UNIFORMLY VALID BANDS FOR THE ORIGINAL MAKAROV BOUNDS
12971298 We now translate the simultaneous bands for the smoothed bounds $\rho_{t_1, t_2}^\pm(\delta)$ into simultaneous bands
1299 for the original Makarov bounds $\rho^\pm(\delta)$. Recall from Lemma 4.1 that
1300

1301
$$\rho_{t_1, t_2}^-(\delta) - b(t_1, t_2) \leq \rho^-(\delta) \quad \text{and} \quad \rho^+(\delta) \leq \rho_{t_1, t_2}^+(\delta) + b(t_1, t_2), \quad (82)$$

1302 for every δ , where
1303

1304
$$b(t_1, t_2) = \frac{\log(2)}{t_2} + \frac{(\log|\mathcal{Y}|)_+}{t_1}$$

1305 does not depend on δ . Hence, the inequalities in (82) hold uniformly for all $\delta \in \Delta$.
13061307 Combining Corollary D.3 with (82) yields the following result.
13081309 **Corollary D.4** (Simultaneous confidence bands for the treatment effect distribution). *Fix $\alpha \in (0, 1)$
1310 and a compact set $\Delta \subset \mathbb{R}$. Let $\hat{c}_{1-\alpha/2}^{-, \text{unif}}$ and $\hat{c}_{1-\alpha/2}^{+, \text{unif}}$ denote the bootstrap critical values obtained as in
1311 Corollary D.3 for the lower and upper smoothed bounds, respectively, with level $\alpha/2$. Define, for
1312 each $\delta \in \Delta$,*

1313
$$\underline{c}_n(\delta) = \hat{\rho}_{t_1, t_2}^-(\delta) - \frac{\hat{c}_{1-\alpha/2}^{-, \text{unif}}}{\sqrt{n}} - b(t_1, t_2), \quad (83)$$

1314
$$\bar{c}_n(\delta) = \hat{\rho}_{t_1, t_2}^+(\delta) + \frac{\hat{c}_{1-\alpha/2}^{+, \text{unif}}}{\sqrt{n}} + b(t_1, t_2). \quad (84)$$

1315 Then
1316

1317
$$\liminf_{n \rightarrow \infty} \mathbb{P}(\forall \delta \in \Delta : \underline{c}_n(\delta) \leq \rho(\delta) \leq \bar{c}_n(\delta)) \geq 1 - \alpha.$$

1318 In particular, the pair of bands $\{\underline{c}_n(\delta)\}_{\delta \in \Delta}$ and $\{\bar{c}_n(\delta)\}_{\delta \in \Delta}$ defines an asymptotically valid $(1 - \alpha)$
1319 simultaneous confidence band for the treatment effect distribution $\rho(\delta)$ uniformly over $\delta \in \Delta$.
13201321 **Practical implementation.** In practice, the set Δ is approximated by a finite grid $\{\delta_1, \dots, \delta_K\} \subset$
1322 Δ . The procedure then reduces to:
13231324 1. Compute $\hat{\rho}_{t_1, t_2}^\pm(\delta_k)$ and $\hat{\psi}_i^\pm(\delta_k)$ for all $k = 1, \dots, K$.
1325 2. For each bootstrap replication $b = 1, \dots, B$, draw multipliers $\{\xi_i^{(b)}\}_{i=1}^n$ and form

1326
$$\hat{G}_{n,b}^{\pm,*}(\delta_k) = \frac{1}{\sqrt{n}} \sum_{i=1}^n \xi_i^{(b)} (\hat{\psi}_i^\pm(\delta_k) - \bar{\hat{\psi}}_n^\pm(\delta_k)),$$

1327 and set $T_{n,b}^{\pm,*} = \max_{k=1, \dots, K} |\hat{G}_{n,b}^{\pm,*}(\delta_k)|$.
13281329 3. Let $\hat{c}_{1-\alpha/2}^{\pm, \text{unif}}$ be the empirical $(1 - \alpha/2)$ quantiles of $\{T_{n,b}^{\pm,*}\}_{b=1}^B$, and construct $\underline{c}_n(\delta_k)$ and
1330 $\bar{c}_n(\delta_k)$ as in (83)–(84).
13311332 For a sufficiently dense grid, the resulting discrete bands provide an accurate approximation to the
1333 uniform confidence bands over Δ .
13341335
1336
1337
1338
1339
1340
1341
1342
1343
1344
1345
1346
1347
1348
1349

1350 **E EXTENSION TO MULTIVALUED TREATMENTS**
13511352 In this appendix, we briefly describe how our methodology extends to settings with multivalued
1353 treatments. Let the treatment take values in a finite set $\mathcal{A} \subset \mathbb{R}$ with $|\mathcal{A}| \geq 2$, and let
1354

1355
$$Z = (X, A, Y) \sim \mathbb{P}, \quad A \in \mathcal{A},$$

1356

1357 where $X \in \mathcal{X} \subseteq \mathbb{R}^d$ and $Y \in \mathbb{R}$ as in the main text. For each $a \in \mathcal{A}$ we denote the potential outcome
1358 by $Y(a)$ and define the generalized propensity scores and response distributions by
1359

1360
$$\pi_a(x) = \mathbb{P}(A = a | X = x), \quad F_a(y | x) = \mathbb{P}(Y \leq y | X = x, A = a).$$

1361

1362 **E.1 TARGET ESTIMAND FOR A PAIR OF TREATMENT LEVELS**
13631364 In many applications, the primary goal is to compare two specific treatment levels $a_1, a_0 \in \mathcal{A}$. For
1365 any such ordered pair (a_1, a_0) we define the treatment effect distribution
1366

1367
$$\rho_{a_1, a_0}(\delta) = \mathbb{P}(Y(a_1) - Y(a_0) \leq \delta), \quad \delta \in \mathbb{R}. \quad (85)$$

1368

1369 This is directly analogous to the binary-treatment estimand in the main text, where $(a_1, a_0) = (1, 0)$.
1370 Under the natural multivalued analogue of Assumption 3.1, namely:
13711372

1. *Consistency*: $Y(a) = Y$ whenever $A = a$ for all $a \in \mathcal{A}$,

1373 2. *Overlap*: $0 < \pi_a(X) < 1$ almost surely for all $a \in \mathcal{A}$,

1374 3. *Ignorability*: $A \perp \{Y(a) : a \in \mathcal{A}\} | X$,

1375 the treatment effect distribution $\rho_{a_1, a_0}(\delta)$ is again partially identified by Makarov-type bounds based
1376 on the pair of marginals (F_{a_1}, F_{a_0}) :
1377

1378
$$\rho_{a_1, a_0}^-(\delta) \leq \rho_{a_1, a_0}(\delta) \leq \rho_{a_1, a_0}^+(\delta), \quad (86)$$

1379

1380 where, for each fixed pair (a_1, a_0) ,
1381

1382
$$\rho_{a_1, a_0}^-(\delta) = \mathbb{E} \left[\sup_{y \in \mathcal{Y}} (F_{a_1}(y | X) - F_{a_0}(y - \delta | X))_+ \right], \quad (87)$$

1383 and
1384

1385
$$\rho_{a_1, a_0}^+(\delta) = 1 + \mathbb{E} \left[\inf_{y \in \mathcal{Y}} (F_{a_1}(y | X) - F_{a_0}(y - \delta | X))_- \right], \quad (88)$$

1386 which are obtained by replacing F_1 and F_0 in Eq. (3) with F_{a_1} and F_{a_0} .
1387

1388 **E.2 REDUCTION TO THE BINARY CASE**
13891390 Our proposed estimators and theoretical results for the binary-treatment case extend directly to this
1391 multivalued setting by a simple recoding argument. For a fixed pair (a_1, a_0) , define the binary
1392 indicators
1393

1394
$$\tilde{A}_{a_1, a_0} = \mathbf{1}\{A = a_1\}, \quad 1 - \tilde{A}_{a_1, a_0} = \mathbf{1}\{A = a_0\},$$

1395 and the corresponding generalized propensity scores
1396

1397
$$\pi_{a_1}(X) = \mathbb{P}(A = a_1 | X), \quad \pi_{a_0}(X) = \mathbb{P}(A = a_0 | X).$$

1398

1399 Conditional on X , the distribution of $(\tilde{A}_{a_1, a_0}, Y)$ restricted to the subset $\{A \in \{a_1, a_0\}\}$ is alge-
1400 braically identical to the binary-treatment setup in the main text with treatment $A = 1$ and control
1401 $A = 0$, after replacing:
1402

1403
$$A \rightsquigarrow \mathbf{1}\{A = a_1\}, \quad 1 - A \rightsquigarrow \mathbf{1}\{A = a_0\}, \quad \pi(X) \rightsquigarrow \pi_{a_1}(X), \quad 1 - \pi(X) \rightsquigarrow \pi_{a_0}(X),$$

1404 and
1405

1406
$$F_1(\cdot | X) \rightsquigarrow F_{a_1}(\cdot | X), \quad F_0(\cdot | X) \rightsquigarrow F_{a_0}(\cdot | X).$$

1404 E.3 INFLUENCE FUNCTIONS AND DEBIASED ESTIMATORS
14051406 Let $\rho_{a_1, a_0, t_1, t_2}^{\pm}(\delta)$ denote the smoothed Makarov bounds obtained by applying the smoothing con-
1407 struction from Lemma 4.1 to (F_{a_1}, F_{a_0}) instead of (F_1, F_0) . The corresponding efficient influence
1408 functions follow by the same substitutions in Theorem 4.2.1409 *Remark E.1* (EIF for multivalued treatments). Fix $a_1, a_0 \in \mathcal{A}$ and define

1410
$$d_{a_1, a_0, \delta, \eta}(y | X) = F_{a_1}(y | X) - F_{a_0}(y - \delta | X),$$

1411

1412 and $I_{t, \delta}^{(a_1, a_0)}(x)$, $w_{t_1, \delta}^{(a_1, a_0)}(y | x)$, $\sigma_{t_1, t_2, \delta}^{\pm, (a_1, a_0)}(x)$ analogously to $I_{t, \delta}(x)$, $w_{t_1, \delta}(y | x)$ and $\sigma_{t_1, t_2, \delta}^{\pm}(x)$
1413 in Theorem 4.2, but with F_1, F_0 replaced by F_{a_1}, F_{a_0} . Then the efficient influence functions for the
1414 smoothed multivalued bounds $\rho_{a_1, a_0, t_1, t_2}^{\pm}(\delta)$ are obtained from Theorem 4.2 by replacing
1415

1416
$$A \rightarrow \mathbf{1}\{A = a_1\}, \quad 1 - A \rightarrow \mathbf{1}\{A = a_0\}, \quad \pi(X) \rightarrow \pi_{a_1}(X), \quad 1 - \pi(X) \rightarrow \pi_{a_0}(X), \quad F_1 \rightarrow F_{a_1}, \quad F_0 \rightarrow F_{a_0}.$$

1417

1418 In particular, the debiased estimators in Eq. (19) extend verbatim to the comparison of any pair
1419 (a_1, a_0) after making these substitutions.1420 Because the derivation of the EIF in Theorem 4.2 relies only on the binary nature of the comparison
1421 (treated vs. control) and not on the cardinality of \mathcal{A} , the same arguments imply that all results
1422 on asymptotic normality, confidence intervals, and uniform confidence bands (Corollary 4.3 and
1423 Appendix D) carry over to the multivalued setting for any fixed pair (a_1, a_0) .1424 In practice, a practitioner who wishes to compare the treatment levels a_1 and a_0 simply specifies
1425 these two values and applies our binary-treatment procedure to the recoded data with A replaced by
1426 $\mathbf{1}\{A = a_1\}$ and the nuisance functions (F_1, F_0, π) replaced by $(F_{a_1}, F_{a_0}, \pi_{a_1})$ and π_{a_0} , as described
1427 above.

1428

1429

1430

1431

1432

1433

1434

1435

1436

1437

1438

1439

1440

1441

1442

1443

1444

1445

1446

1447

1448

1449

1450

1451

1452

1453

1454

1455

1456

1457

1458 F DETAILS ON NUISANCE ESTIMATION
14591460 We estimate the response c.d.f.s $F_a(y | x)$, $a \in \{0, 1\}$, by fitting separate conditional distribution
1461 models within each arm ($A = a$). All learners return the *entire* conditional c.d.f. evaluated on an
1462 arbitrary grid $y \in \mathcal{Y}$, which is required by the EIF in (4.2).
14631464 **Training protocol (common to all learners).** For each arm a we split the data into two folds
1465 as outlined in Algorithm 1. On each fold, we train on the complement and predict $\hat{F}_a(\cdot | x_i)$ for
1466 held-out i . Models are trained by gradient boosting (LightGBM) with early stopping on a validation
1467 set and a likelihood-based metric. Monotone transformations T of Y can be applied for numerical
1468 stability; since T is monotone, $F_Y(y | x) = F_{T(Y)}(T(y) | x)$. In particular, we use standardization
1469 and log-transformation where appropriate. Given a grid $\{y_j\}_{j=1}^J$, each learner returns the matrix
1470 $(\hat{F}_a(y_j | x_i))_{i,j}$. These values feed the smoothed operators in (9) and the weighted integrals
1471 $\hat{\Phi}_{t_1, \delta}^a(x_i, y_i)$ in (19).
14721473 **Continuous outcomes: conditional Gaussian mixtures.** For $Y \in \mathbb{R}$ we model $T(Y) | X = x$
1474 as a K -component Gaussian mixture with covariate-dependent weights $\pi_k(x)$, means $\mu_k(x)$ and
1475 variances $\sigma_k^2(x)$. Boosting optimizes the (negative) log-likelihood with a custom objective
1476

1477
$$\ell_{\text{GM}}(x, y) = -\log \left(\sum_{k=1}^K \pi_k(x) \varphi(T(y); \mu_k(x), \sigma_k^2(x)) \right),$$

1478
1479

1480 where $\varphi(y; \mu, \sigma^2)$ is the $\mathcal{N}(\mu, \sigma^2)$ density. The log-likelihood loss supplies per-parameter gradients
1481 and diagonal Hessians. Derivatives are rescaled to balance curvature across logits/means/variances.
1482 Initialization uses k -means on $T(Y)$ (cluster means/variances feed the intial score matrix. The
1483 resulting c.d.f. is

1484
$$\hat{F}_a(y | x) = \sum_{k=1}^K \hat{\pi}_k(x) \Phi \left(\frac{T(y) - \hat{\mu}_k(x)}{\hat{\sigma}_k(x)} \right).$$

1485
1486

1487 **Discrete outcomes: multinomial classifier.** For discrete Y taking finitely many values $\{c_1 < \dots < c_M\}$ we fit a multiclass boosted classifier returning $\hat{p}_x(c_m) = \Pr(Y = c_m | X = x)$. The
1488 c.d.f. is the cumulative sum
1489

1490
$$\hat{F}_a(y | x) = \sum_{m: c_m \leq y} \hat{p}_x(c_m),$$

1491
1492

1493 implemented by summing predicted class probabilities over classes $\leq y$.
14941495 **Counts with excess zeros: zero-inflated Poisson (ZIP).** For nonnegative counts we fit a covariate-
1496 dependent ZIP with rate $\lambda(x)$ and zero-inflation $\psi(x)$, learned via a custom objective for the ZIP
1497 log-likelihood and stabilized derivatives. Initialization uses the empirical mean for λ and the observed
1498 zero rate for ψ . The c.d.f. (right-continuous) is
1499

1500
$$\hat{F}_a(y | x) = \begin{cases} 0, & y < 0, \\ \psi(x) + (1 - \psi(x)) \text{PoisCDF}(\lfloor y \rfloor; \lambda(x)), & y \geq 0. \end{cases}$$

1501
1502
1503
1504
1505
1506
1507
1508
1509
1510
1511

1512 **G DETAILS REGARDING SYNTHETIC DATA**
 1513

1514 **Data generating process.**
 1515

1516 We sample uniform covariates $X \sim \text{Unif}[0, 1]$ and define $\rho(x) = \frac{1}{2}x^2 + \frac{1}{2}$. We then define the
 1517 c.d.f. for the treatment arm as

$$1518 \quad 1519 \quad 1520 \quad 1521 \quad 1522 \quad Y(1) \mid X = x \sim \text{Unif}([0, \rho(x)]), \quad F_{1|x}(y) = \begin{cases} 0, & y < 0, \\ \frac{y}{\rho(x)}, & 0 \leq y \leq \rho(x), \\ 1, & y > \rho(x). \end{cases}$$

1523 For the control arm, we define for a parameter γ

$$1524 \quad 1525 \quad L_1(x) = -\frac{\gamma}{4}x, \quad L_2(x) = \frac{1}{2}\rho(x) + \frac{\gamma}{4}x.$$

1526 Then, we define the control arm c.d.f. as
 1527

$$1528 \quad 1529 \quad 1530 \quad 1531 \quad 1532 \quad 1533 \quad 1534 \quad 1535 \quad 1536 \quad F_{0|x}(y) = \begin{cases} 0, & y < L_1, \\ \frac{y - L_1}{\rho}, & L_1 \leq y \leq L_1 + \frac{1}{2}\rho, \\ \frac{1}{2}, & L_1 + \frac{1}{2}\rho < y < L_2, \\ \frac{1}{2} + \frac{y - L_2}{\rho}, & L_2 \leq y \leq L_2 + \frac{1}{2}\rho, \\ 1, & y > L_2 + \frac{1}{2}\rho, \end{cases}$$

1537 where, for brevity, $L_j = L_j(x)$ and $\rho = \rho(x)$. The gap between the two control components is
 1538

$$1539 \quad G(x) = L_2 - \left(L_1 + \frac{1}{2}\rho \right) = \frac{\gamma}{2}x.$$

1541 To model a joint distribution leveraging the marginals above, we draw (U_1, U_0) from a Gumbel
 1542 copula C_θ with $\theta = 5$ (dimension 2), and set
 1543

$$1544 \quad Y(1) \mid X = F_{1|x}^{-1}(U_1), \quad Y(0) \mid X = F_{0|x}^{-1}(U_0).$$

1545 Finally, the observed outcome is $Y = A Y(1) + (1 - A) Y(0)$.
 1546

1547 **Quantifying margin violation.** The difference $D_x(y) = F_{1|x}(y) - F_{0|x}(y)$ admits two plateaus that
 1548 attain supremum and infimum and thus violating the margin assumption. The left, negative one is
 1549 given for $0 \leq y \leq \frac{1}{2}\rho - \frac{\gamma}{4}x$ as

$$1550 \quad 1551 \quad 1552 \quad D_x(y) = \frac{y}{\rho} - \frac{y - L_1}{\rho} = \frac{L_1}{\rho} = -\frac{\gamma x}{4\rho}.$$

1553 Its width is
 1554

$$W_L(x) = \frac{\rho}{2} - \frac{\gamma}{4}x.$$

1555 The right, positive plateau is given for $\frac{1}{2}\rho + \frac{\gamma}{4}x \leq y \leq \rho$ as
 1556

$$1557 \quad 1558 \quad 1559 \quad D_x(y) = \frac{y}{\rho} - \left(\frac{1}{2} + \frac{y - L_2}{\rho} \right) = \frac{L_2 - \frac{1}{2}\rho}{\rho} = +\frac{\gamma x}{4\rho}.$$

1560 Its width is given by
 1561

$$W_R(x) = \frac{\rho}{2} - \frac{\gamma}{4}x.$$

1563 Averaging over X yields $\mathbb{E}[\rho(X)] = \frac{2}{3}$, $\mathbb{E}[X] = \frac{1}{2}$, and
 1564

$$1565 \quad \mathbb{E}\left[\frac{X}{\rho(X)}\right] = \int_0^1 \frac{2x}{x^2 + 1} dx = \ln 2.$$

1566 Hence, obtain average plateau widths
 1567

$$1568 \quad \mathbb{E}[W_L(X)] = \mathbb{E}[W_R(X)] = \frac{1}{3} - \frac{\gamma}{8}, \quad \mathbb{E}[G(X)] = \frac{\gamma}{4}, \\ 1569$$

1570 and normalized

$$1571 \quad \mathbb{E}\left[\frac{W_L(X)}{\rho(X)}\right] = \mathbb{E}\left[\frac{W_R(X)}{\rho(X)}\right] = \frac{1}{2} - \frac{\gamma}{4} \ln 2, \quad \mathbb{E}\left[\frac{G(X)}{\rho(X)}\right] = \frac{\gamma}{2} \ln 2. \\ 1572 \\ 1573$$

1574 Thus, when decreasing γ , we maximize the average plateau width and correspondingly the degree
 1575 of margin violation.

1576

1577

1578

1579

1580

1581

1582

1583

1584

1585

1586

1587

1588

1589

1590

1591

1592

1593

1594

1595

1596

1597

1598

1599

1600

1601

1602

1603

1604

1605

1606

1607

1608

1609

1610

1611

1612

1613

1614

1615

1616

1617

1618

1619

1620 H DETAILS REGARDING SEMI-SYNTHETIC DATA

1622 **Real-world covariate data.** The so-called *Oregon health insurance experiment*² (OHIE) (Finkelstein
 1623 et al., 2012) is a randomized experiment that was intentionally conducted as a large-scale effort in
 1624 public health to assess the effect of health insurance on several outcomes such as health or economic
 1625 status. In 2008, a lottery draw offered low-income, uninsured adults in Oregon participation in a
 1626 Medicaid program, providing health insurance. Individuals whose names were drawn could decide to
 1627 sign up for the program.

1628 In our analysis, we extract the following covariates X : age, gender, language, the number of
 1629 emergency visits before the experiment, and the number of people the individual signed up with.
 1630 The data collection in the OHIE was done as follows: after excluding individuals below the age
 1631 of 19, above the age of 64, and individuals with residence outside of Oregon, 74,922 individuals
 1632 were considered for the lottery. Among those, 29,834 were selected randomly and were offered
 1633 participation in the program. Out of these, we randomly select $n = 3000$ data points.

1634 **Synthetic treatment and outcome generation.** We define the empirical mean covariate

$$1636 \quad m(x) = \frac{1}{p} \sum_{j=1}^p x_j.$$

1639 and introduce two covariate-dependent shape functions:

$$1640 \quad \rho(x) = \frac{1}{2} m(x)^2 + \rho_0, \quad g(x) = m(x)^3,$$

1642 where $\rho_0 > 0$ is a constant hyperparameter (in our experiments $\rho_0 = 0.5$). The treatment is
 1643 randomized with constant propensity:

$$1644 \quad \pi(x) \equiv \mathbb{P}(A = 1 \mid X = x) = \frac{1}{2}, \quad A_i \sim \text{Bernoulli}\left(\frac{1}{2}\right) \text{ independently of } X_i.$$

1646 We define the treatment c.d.f. as

$$1648 \quad Y(1) \mid X = x \sim \text{Unif}([0, \rho(x)]), \quad F_{1|x}(y) = \begin{cases} 0, & y < 0, \\ \frac{y}{\rho(x)}, & 0 \leq y \leq \rho(x), \\ 1, & y > \rho(x). \end{cases}$$

1652 For the control arm c.d.f., we define

$$1654 \quad L_1(x) = -\frac{1}{4} g(x), \quad L_2(x) = \frac{1}{2} \rho(x) + \frac{1}{4} g(x),$$

1655 and

$$1656 \quad F_{0|x}(y) = \begin{cases} 0, & y < L_1, \\ \frac{y - L_1}{\rho}, & L_1 \leq y \leq L_1 + \frac{1}{2}\rho, \\ \frac{1}{2}, & L_1 + \frac{1}{2}\rho < y < L_2, \\ \frac{1}{2} + \frac{y - L_2}{\rho}, & L_2 \leq y \leq L_2 + \frac{1}{2}\rho, \\ 1, & y > L_2 + \frac{1}{2}\rho, \end{cases}$$

1665 where, for brevity, $L_j = L_j(x)$ and $\rho = \rho(x)$.

1667 To couple $Y(1)$ and $Y(0)$ while preserving the marginals above, we draw (U_1, U_0) from a Gumbel
 1668 copula C_θ with $\theta = 5$ (dimension 2), and set

$$1669 \quad Y(1) = F_{1|x}^{-1}(U_1), \quad Y(0) = F_{0|x}^{-1}(U_0).$$

1671 Finally, the observed outcome is $Y = A Y(1) + (1 - A) Y(0)$.

1673 ²Data available here: <https://www.nber.org/programs-projects/projects-and-centers/oregon-health-insurance-experiment>

1674
 1675 **Quantifying margin violations.** The c.d.f. difference $D_x(y) = F_{1|x}(y) - F_{0|x}(y)$ again admits two
 1676 plateaus attaining the supremum and infimum, thus violating the margin assumption for both lower
 1677 and upper bound.

1678 For $0 \leq y \leq \frac{1}{2}\rho - \frac{1}{4}g$, the left plateau is

$$1679 \quad D_x(y) = \frac{y}{\rho} - \frac{y - L_1}{\rho} = \frac{L_1}{\rho} = -\frac{g}{4\rho},$$

1680 with an associated width of $W_L(x) = \frac{\rho}{2} - \frac{g}{4}$.

1681
 1682 For $\frac{1}{2}\rho + \frac{1}{4}g \leq y \leq \rho$, the right plateau is

$$1683 \quad D_x(y) = \frac{y}{\rho} - \left(\frac{1}{2} + \frac{y - L_2}{\rho}\right) = \frac{L_2 - \frac{1}{2}\rho}{\rho} = +\frac{g}{4\rho}.$$

1684 with a width of $W_R(x) = \frac{\rho}{2} - \frac{g}{4}$. The average widths are given via

$$1685 \quad \mathbb{E}[W_L(X)] = \mathbb{E}[W_R(X)] = \mathbb{E}\left[\left(\frac{1}{2}\rho_0 + \frac{1}{4}(m(X)^2 - m(X)^3)\right)_+\right].$$

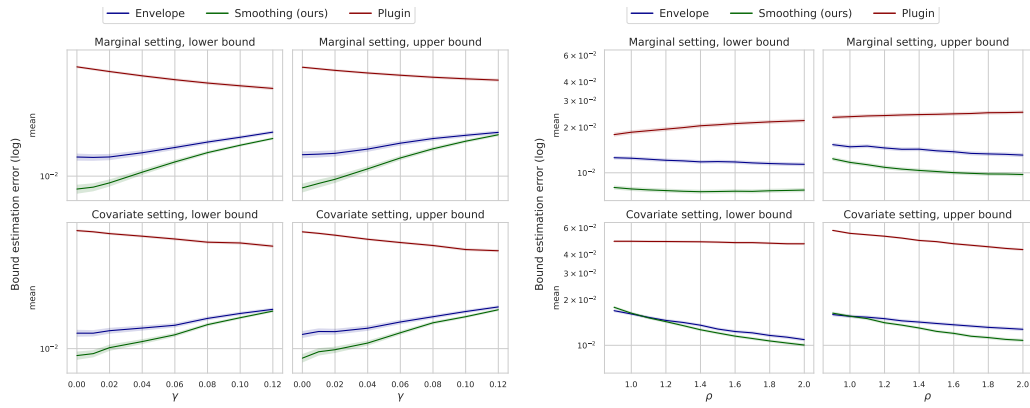
1686 Hence, the widths of the plateaus and thus also the degrees of margin violations increasing in ρ_0 .

1687
 1688
 1689
 1690
 1691
 1692
 1693
 1694
 1695
 1696
 1697
 1698
 1699
 1700
 1701
 1702
 1703
 1704
 1705
 1706
 1707
 1708
 1709
 1710
 1711
 1712
 1713
 1714
 1715
 1716
 1717
 1718
 1719
 1720
 1721
 1722
 1723
 1724
 1725
 1726
 1727

1728 I ADDITIONAL EXPERIMENTS

1730 I.1 (SEMI)-SYNTHETIC DATA

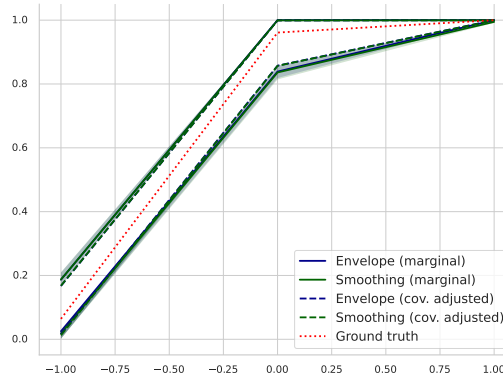
1732 Here, we report full results for the synthetic and semi-synthetic datasets from Appendix G and
 1733 Appendix H for a range of parameters γ (synthetic) and ρ (semi-synthetic) to complement the results
 1734 from Table 2. Recall that increasing γ *decreases* margin violation, while higher ρ *increase* margin
 1735 violation. The results for all methods are bound types are reported in Fig.3. For both datasets, larger
 1736 margin violation leads to a larger gap between our method and the baselines. Importantly, **our**
 1737 **method consistently outperforms the baselines.**



1752 Figure 3: Results for synthetic and semi-synthetic data over a range of parameters quantifying margin
 1753 violation.

1754 I.2 TWINS DATASET

1756 Here, we use the binary outcome TWINS dataset from Louizos et al. (2017). The covariates X are
 1757 measurements and demographic attributes of various twin pairs below 2000 grams. The treatment A
 1758 is being born as the heavier twin, and the outcome Y denotes infant mortality within the first year
 1759 of life. As both counterfactual outcomes are observed, we can estimate the ground-truth treatment
 1760 effect c.d.f. , which we plot along the estimated Makarov bounds in Fig.4. We see that the estimated
 1761 bounds are tight and cover the ground-truth treatment effect c.d.f. , thus confirming the validity of our
 1762 estimator.



1775 Figure 4: Estimated bounds and treatment effect c.d.f. for the TWINS dataset.

1778 I.3 ADDITIONAL RESULTS FOR CONSUMER COMPANY A/B TESTS

1780 In Figure 5, we compare both the results of our smoothed estimator with the results of the envelope
 1781 baseline. The upper Makarov bound estimates mostly coincide, however, our estimator is more
 conservative and estimates a smaller lower bound than the baseline. As our estimator is obtained by

1782 minimizing MSE over various smoothing parameters (including the special case of large smoothing
 1783 parameters coinciding with the envelope), this indicates that the ground-truth Makarov bound is
 1784 smaller than the envelope estimate. In particular, this may indicate envelope estimator is too confident
 1785 and may undercover the ground-truth treatment effect c.d.f. , leading to potentially wrong conclusions.
 1786

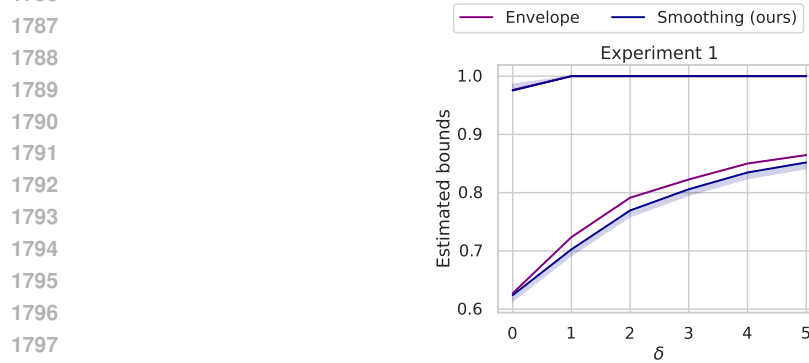


Figure 5: Estimated bounds and confidence intervals for Experiment 1.